SUBSURFACE STORMWATER RETENTION WITH PERVIOUS CONCRETE PAVEMENT ON UPRM CAMPUS MASTER PLAN

By

CARLA M. MORENO CORTÉS

A thesis submitted in partial fulfillment of the requirements for the degree of

MASTER IN SCIENCE

IN

CIVIL ENGINEERING

(Environmental and Water Resources Engineering)

UNIVERSITY OF PUERTO RICO

MAYAGÜEZ CAMPUS

2018

Approved by:

Sangchul S. Hwang, PhD President, Graduate Committee	Date
Alesandra C. Morales Vélez, PhD Member, Graduate Committee	Date
Enrique González Vélez, PhD Member, Graduate Committee	Date
Víctor Huérfano, PhD Representative, Graduate School	Date
Ismael Pagán Trinidad, MSCE Chair, Department of Civil Engineering and Surveying	Date

ABSTRACT

Pervious concrete pavement constitutes an efficient Best Management Practice (BMP) stormwater management solution, since it serves to manage surface runoff quantitative and qualitative characteristics at its earliest stages. Since flash flooding occurs very often on campus of the University of Puerto Rico at Mayagüez (UPRM) under a normal rain event, the use of pervious concrete, results in the conservation and protection of water resources by leading to the reduction of flooding events downstream, non-point source pollutant transport, and on-site ponding. In order to implement the pervious concrete BMP system, a sustainability assessment was performed to identify possible sites in need of this practice, equipped with a subsurface water retention structure, hydrologic design, estimation of construction costs and resulting reduction of stormwater runoff volume.

The sustainability assessment was done with a Multi-criteria Decision Analysis (MCDA) in conjunction with the Analytic Hierarchy Process (AHP) approach. The AHP approach, evaluated three sustainability categories, which are social, economic and environmental. Each one was ranked based on a particular and specific criteria, which was developed considering the input collected from a group of ten experts who were asked to fill a questionnaire comparing the different criteria under each sustainability category. These experts input was served to establish the ranking values for the criteria, resulting in the selection of social sustainability as the one with the highest value. Additionally, from the on site assessment of the campus, seven critical areas identified and the Mangual/Terrace and Faculty Building were identified as the ones in the most need of a PC system with overall ranked values of 4.1 and 4.0, respectively. Once the areas were identified, a study was made to attain an optimized mortar mixture incorporating glass and fly ash as partial replacement of cement. Since the main focus of the project is to incorporate sustainability in all aspects as possible, and given the lack of glass recycling and high quantities of fly ash that end up at landfills in P.R., the incorporation of both as construction materials was studied. X-ray diffraction (XRD) and a hydrometer test were also performed to analyze the chemical composition of the glass and the particle size distribution respectively. XRD revealed an amorphous pattern on the glass powder while the hydrometer test results showed that the cumulative measure for 50% of particles size was 8 µm. The optimization of the mixture was done using Response Surface Methodology (RSM) to get the highest possible compressive

strength value with a targeted spread percentage of 110%. At 28 days of curing, the optimum values for a maximum compressive strength of 83 MPa and 110 spread percentage were 7.25% glass-to-binder ratio (G/B) and 14.30% fly ash-to-binder ratio (FA/B).

After obtaining an optimized mix mortar containing glass powder and fly ash, it was incorporated to pervious concrete (PC). Because permeability and compressive strength are both important mechanical properties for PC and are inversely proportional to each other, a good balance between them is essential to attain the ideal design of PC. The measured values for compressive strength and permeability fell within the typical values specified by the National Ready Mix Concrete Association (NRMCA) and the American Concrete Institute (ACI). Since all the areas to be analyzed have different characteristics, for the implementation of the PC, the designs must be developed specifically for the selected area. Correspondingly, a hydrological study was carried out for the different areas in need of a pervious concrete system. The study was done using the National Resources Conservation Service (NRCS) method with a rainfall recurrence of 2 years and duration of 24 hours. Results of the analysis allowed evaluating the excess of runoff before and after the implementation of a PC system. A soil study was also performed on the Mangual/Terrace area to evaluate the soil properties specific to the site. The result from both studies allowed for the creation of a PC design that takes into consideration the site-specific characteristics. Furthermore, the design served not only as a stormwater subsurface storage structure but it also encompassed the safety of the students through a bicycle lane that would enhance the students' daily commute.

RESUMEN

El pavimento de concreto permeable constituye una solución eficiente de las Mejores Prácticas de Manejo (BMP por sus siglas en inglés) para el manejo de agua de escorrentía, ya que sirve para gestionar las características cuantitativas y cualitativas de la escorrentía superficial en sus primeras etapas. Dado a que los eventos de inundaciones repentinas ocurren muy a menudo en la Universidad de Puerto Rico en Mayagüez (UPRM), el uso de concreto permeable resulta en la conservación y protección de los recursos hídricos ya que ayuda a reducir las inundaciones aguas abajo, el transporte de contaminantes no puntuales y el estancamiento. Se realizó una evaluación de sustentabilidad para identificar posibles sitios en necesidad de la implementación de un sistema de concreto permeable. Este sistema está equipado con una estructura de retención de agua subterránea, diseño hidrológico, estimación de costos de construcción y el resultado en la reducción del volumen de escorrentía de aguas pluviales.

La evaluación de sustentabilidad se realizó con un Análisis de Decisión Multi-criterio (MCDA por sus siglas en inglés) junto con el enfoque del Proceso Analítico de Jerarquía (AHP por sus siglas en inglés). El enfoque AHP evaluó tres categorías de sustentabilidad que son la social, económica y ambiental. Cada una, clasificada según un criterio particular y específico, se desarrolló teniendo en cuenta la información recopilada de un grupo de diez expertos a los que se les pidió que completaran un cuestionario que comparara los diferentes criterios de cada categoría de sustentabilidad. La aportación de estos expertos, sirvió para establecer los rangos de valores de los criterios, lo que resultó en la selección de la sustentabilidad social como la de mayor valor. Además, a partir de la evaluación de campo del recinto, se identificaron siete áreas críticas, de las cuales Mangual/Terrace y el Edificio de Facultad, resultaron como las más necesitadas de un sistema de concreto permeable con valores de 4.1 y 4.0, respectivamente. Una vez identificadas las áreas, se realizó un estudio para obtener una mezcla de mortero óptima que incorpore vidrio y cenizas volantes como reemplazo parcial del cemento. Dado que el objetivo principal del proyecto es incorporar la sustentabilidad en todos los aspectos posibles, y dada la falta de reciclaje de vidrio y altas cantidades de cenizas volantes que terminan en vertederos en P.R., se estudió la incorporación de ambos como materiales de construcción. Se realizaron las pruebas de difracción de rayos X (XRD por sus siglas en inglés) y una prueba de hidrómetro para analizar la composición química del vidrio y la distribución del tamaño de partícula,

respectivamente. El XRD reveló un patrón amorfo en el vidrio, mientras que los resultados de la prueba del hidrómetro mostraron que la medida acumulativa del 50% del tamaño de las partículas fue de 8 μm. La optimización de la mezcla se realizó utilizando la metodología de superficie de respuesta (RSM por sus siglas en inglés) para obtener el valor de resistencia a la compresión más alto posible con un porcentaje de dispersión del 110%. A los 28 días de curado, los valores óptimos para una resistencia máxima a una compresión de 83 MPa y 110% de dispersión fueron de 7.25% de vidrio a proporción de aglutinante (G/B) y 14.30% de ceniza volante a proporción de aglutinante (FA/B).

Después de obtener un mortero de mezcla optimizado que contenía polvo de vidrio y cenizas volantes, se incorporó la misma al concreto permeable (PC por sus siglas en inglés). Debido a que la permeabilidad y la resistencia a la compresión son propiedades mecánicas importantes para el PC y son inversamente proporcionales entre sí, un buen equilibrio entre ellas es esencial para lograr el diseño ideal. Los valores medidos para la resistencia a la compresión y la permeabilidad cayeron dentro de los valores típicos especificados por la National Ready Mix Concrete Association (NRMCA) y el American Concrete Institute (ACI). Dado que todas las áreas a analizar tienen diferentes características, para la implementación del PC, los diseños deben desarrollarse específicamente para el área seleccionada. En consecuencia, se llevó a cabo un estudio hidrológico para las diferentes áreas que necesitan un sistema de concreto permeable. El estudio se realizó utilizando el método del Servicio Nacional de Conservación de Recursos (NRCS por sus siglas en inglés), con una recurrencia de precipitación de 2 años y una duración de 24 horas. Los resultados del análisis permitieron evaluar el exceso de escorrentía antes y después de la implementación de un sistema de PC. También se realizó un estudio de suelo en el área de Mangual/Terrace para evaluar las propiedades del suelo específicas del sitio. El resultado de ambos estudios, permitió la creación de un diseño de PC que tome en cuenta las características específicas del sitio. Además, el diseño sirvió no solo como una estructura de almacenamiento subterránea de aguas pluviales sino que también abarca la seguridad de los estudiantes a través de un carril para bicicletas que mejorará el viaje diario de los estudiantes.

To God, for guiding me through this journey and giving me strength I needed.

To my family for always loving and support me.

To my fiancé for his unconditional love and endless support,

ACKNOWLEDGEMENTS

I would like to greatly thank my advisor Dr. Sangchul Hwang for giving me the opportunity to do this research and be part of the HEDGE team. Thank you for the support and commitment that you have given me during these two years of study. I would also like to thank Dr. Enrique González and Dr. Alesandra Morales for their support during this investigation.

Thanks to the group of graded students and undergraduates who have always been present to help and dedicate their time, Marleisa Arocho, Rafael Terán, Victor Torres, Tatiana Mejías and all other students that in one way or another are part of the HEDGE team. I would also like to thank Perla for her help in the environmental laboratory, Jaime for his help in the soil laboratory and Monse in the materials laboratory.

I would also like to thank the Chancellor's Office of the University of Puerto Rico in Mayaguez and AES PR for the financial support during the period of this investigation. Thanks also to the private industry for supplying materials, equipment and support to carry out this research. Essroc Italcementi Group (now Argos San Juan Cement), AES PR and BASF.

Finally, I want to thank my fiancé for his tireless support during the course of this investigation and for his words of words of encouragement during difficult times. Thanks to my family for always encouraging me to keep going and never give up.

Table of Contents

LIST OF TABLES

LIST OF FIGURES

LIST OF ACRONYMS

ACI – American Concrete Institute

ADS – Autoridad de Desperdicios Sólidos

AHP – Analytic Hierarchy Process

ANOVA – Analysis of Variance

ASR – Alkali-Silica Reaction

ASTM – American Society for Testing and Materials

BMPs – Best Management Practices

CCD – Central Composite Design

CN – Curve Number

C-S-H – Calcium Silicate Hydrate

DEM – Digital Elevation Model

FA – Fly Ash

FA/B – Fly Ash-to-binder ratio

G/B – Glass-to-binder ratio

HSG – Hydrologic Soil Group

LOI – Loss on Ignition

MCDA – Multi Criteria Decision Analysis

NOAA – National Oceanic and Atmospheric Association

NRCS – Natural Resources Conservation Service

NRMCA – National Ready Mix Concrete Association

PC – Pervious Concrete

PCP – Pervious Concrete Pavement

RSM – Response Surface Methodology

SUDS – Sustainable Urban Drainage Systems

UPRM – University of Puerto Rico at Mayagüez

VMA – Viscosity Modifying Admixture

XRD – X-Ray Diffraction

1 INTRODUCTION

1.1 BACKGROUND

Puerto Rico is a small island of about 3,435 square miles (mi^2) located in the Caribbean. It has a tropical climate that reaches a mean annual temperature of 77 °F and its precipitation varies across the island (PRCCC, 2013). The municipality of Mayagüez, located at the western coast of the island, is the main location for the University of Puerto Rico at Mayagüez (UPRM). With a population of more than 12,000 students and employees around campus in recent years (Institutional Office of Research and Planning, 2015), infrastructure development within campus is vital. But while development is important, it is critical to take into account any negative impacts it may cause on stormwater management structures. Urban development replaces permeable surfaces with impervious surfaces, which are typically designed to remove rainfall as quickly as possible. Consequently, by increasing the proportion of paved areas comes a decrease in infiltration and evapotranspiration paths of precipitation, thus increasing the amount of precipitation leaving an area as runoff. In fact, urban development increases the peak runoff rate, decreasing its travel time (US EPA, 1993). During a regular year, Mayagüez will typically experience a dry season from January to July and a wet season from August to December. The annual precipitation is approximately 85.33 inches (NWSF, 2010). Nevertheless, it is very common that almost every day during the afternoons, the UPRM campus experiences some random rain events that can vary from very low to very high intensity. In recent years, particularly in 2011 and 2016, the vast majority of campus underwent flash flooding events that caused interruptions of the daily activities as well as some property damage.

As of 2015, the United Nations (UN), appointed the importance of sustainable development, presenting 17 goals (Table 1.1), from which two of them focuses on the development of sustainable cities and communities and water management. Improved urban planning and management are needed to make the world's urban spaces more inclusive, safe, resilient and sustainable (ECOSOC, 2017). Pervious concrete pavement represents a sustainable development tool since its application provides with stormwater management, runoff pollution control and safety enhancement while simultaneously reduces ponding and its risk of hydroplaning and vector attraction.

Table 1.1: United Nations Sustainable Development Goals

Goal	Description
1	End poverty in all it forms everywhere
2	End hunger, achieve food security and improved nutrition and promote sustainable agriculture
3	Ensure healthy lives and promote well-being for all at all ages
4	Ensure inclusive and equitable quality education and promote lifelong learning opportunities for all
5	Achieve gender equality and empower all women and girls
6	Ensure availability and sustainable management of water and sanitation for all
7	Ensure access to affordable, reliable, sustainable and modern energy for all
8	Promote sustained, inclusive and sustainable economic growth, full and productive employment and decent work for all
9	Build resilient infrastructure, promote inclusive and sustainable industrialization and foster innovation
10	Reduce inequality within and among countries
11	Make cities and human settlements inclusive, safe, resilient and sustainable
12	Ensure sustainable consumption and production patterns
13	Take urgent action to combat climate change and its impacts
14	Conserve and sustainably use the oceans, seas and marine resources for sustainable development
15	Protect, restore and promote sustainable use of terrestrial ecosystems, sustainably manage forests, combat desertification, and halt and reverse land degradation and halt biodiversity loss
16	Promote peaceful and inclusive societies for sustainable development, provide access to justice for all and build effective, accountable and inclusive institutions at all levels
17	Strengthen the means of implementation and revitalize the Global Partnership for Sustainable Development 21.

1.2 JUSTIFICATION

Flash flooding events at the UPRM campus occur very often. As campus development increases, thereby increases the impervious surfaces, altering the natural surface drainage system. Nevertheless without the ability to infiltrate stormwater, local flooding and runoff formation occurs, becoming a high risk to the present surface drainage system. Though, surface drainage systems not always constitute the best drainage alternative. If they receive more water than the design capacity, the stormwater managing structures fail to work, leading to additional problems such as the accumulation of water, creating a breeding ground for disease carrying organisms such as mosquitos (e.g., *Aedes Aegipti* for Zika virus). Furthermore, runoff carries with it the pollutants deposited on the surface that ultimately end up in water bodies. Sustainable drainage techniques have emerged as a set of systems that reproduce the natural processes of water management. Their purpose was to mitigate the peak flow volumes of runoff and reduce water pollution by implementing mechanisms of infiltration, transport and retention. The initial development occurred in USA during the 1970s with the name of Best Management Practices (BMPs) (Castro-Fresno et al., 2013). Stormwater BMP is a technique, measure, or structural control that is used to manage the quantity and improve the quality of stormwater runoff in the most cost effective manner (US EPA, 2004). Pervious concrete constitute in an efficient BMP solution since it directly manages surface runoff quantitative and qualitative at its earliest stages, due to the synergistic action of its pervious layers. Such layers allow the infiltration into the pervious concrete system that can alternatively serve as a storage, recycling and conveyance of surface water (Pratt et al., 2002). For this project, it is proposed to perform a sustainability assessment that will serve as a tool to develop a UPRM Campus Master Plan. It is also important to mention that the livability and safety of students and employees on campus will get enhanced through a more sustainable-engineered ecosystem. Furthermore, this development will achieve the conservation and protection of water resources by the application of BMPs that will lead to the reduction of flash flooding downstream, non-point source pollutant transport and on-site ponding. The assessment will include the identification of possible sites in need of a pervious concrete pavement system, equipped with a subsurface water retention structure, hydrologic design, estimation of construction costs and resulting reduction of stormwater runoff volume. In view of the fact that the resultant alternatives should denote an objective identification, a Multi-Criteria Decision Analysis (MCDA) was used.

1.3 OBJECTIVES

The aim of this research is to develop a master plan for the UPRM campus for the implementation of a subsurface stormwater retention structure with pervious concrete pavement. In order to meet the aforementioned main goal of this research, a series of tasks were carried out which covered the following:

(1) The use of the AHP approach as an MCDA tool;

(2) A thorough assessment of potentially impacted areas within the UPRM campus; and

(3) The specific design of a pervious concrete system for the resultant area in most need of a stormwater management subsurface structure.

1.4 LITERATURE REVIEW

1.4.1 Sustainability

Water is a finite resource that is fundamental to human well-being and only renewable if well managed. Smart water management is a pre-condition of sustainable development. Managed efficiently, water plays a vital role in strengthening the resilience of social, economic and environmental systems in the face of rapid and unpredictable changes (Bogena, 2015). Figure 1.1 represents these dimensions as nested, with a resilient and robust economy existing within a healthy society dependent on an intact and functional environment (US EPA, 2017).

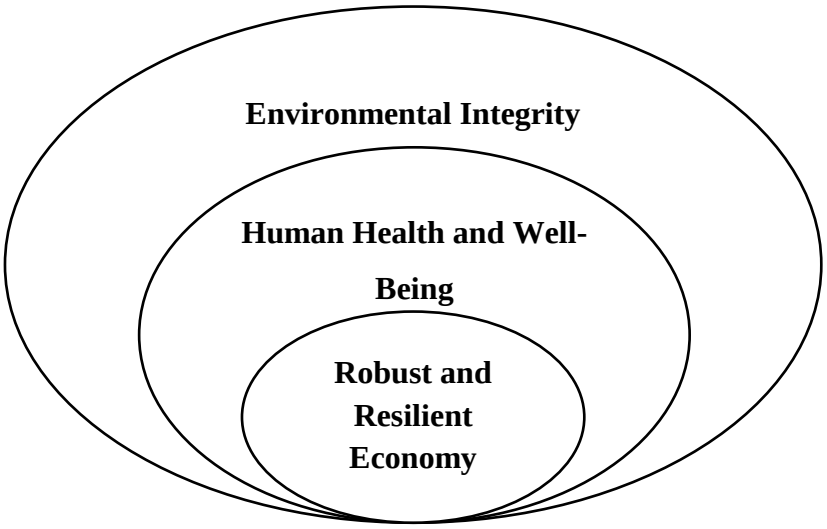

Figure 1.1: Economy, Social and Environment: A nested relationship (Source: US EPA, 2017)

The concept of triple-bottom-line captures the spectrum of values that a Sustainable Urban Drainage System must embrace, the economic, environmental, and social dimensions. Decision-making about urban water infrastructure projects is complex. There may be an array of available infrastructural and technological options to choose between. Decisions need to account for interdependencies between existing infrastructures, complex hydrologic, economic, environmental, financial, institutional, and social conditions, and water, land and energy use constraints. The very unique local characteristics and requirements of any water management project mean that no single combination can be recommended as a panacea (Wilcox et al., 2016).

1.4.1.1 Social Sustainability

Social sustainability can be defined as a condition and a process that improves a community's quality of life (Colantonio, 2011). An infrastructure project contributes to sustainability in the short and long term, which can be measured using social improvement criteria and goals, respectively (Sierra et al., 2017). The criteria are requirements to an intervention that must be fulfilled to obtain a sustainability standard (Pavlovskaia, 2013).

1.4.1.2 Economic Sustainability

Economic sustainability' implies a system of production that satisfies present consumption levels without compromising future needs. The sustainability that economic sustainability seeks is the sustainability of the economic system itself. Traditionally, economists, assuming that the supply of natural resources was unlimited, placed undue emphasis on the capacity of the market to allocate resources efficiently. They also believed that economic growth would bring the technological capacity to replenish natural resources destroyed in the production process. Today, however, a realization has emerged that natural resources are not infinite. The growing scale of the economic system has strained the natural resource base (Basiago, 1999).

1.4.1.3 Environmental Sustainability

Environmental Sustainability involves ecosystem integrity, carrying capacity and biodiversity. It requires that natural capital be maintained as a source of economic inputs and as a sink for wastes. Resources must be harvested no faster than they can be regenerated. Wastes must be emitted no faster than the environment can assimilate them (Khan, 1995).

1.4.2 Multi-Criteria Decision Analysis (MCDA)

With the ever-increasing awareness of urban environment protection and pursuit of high quality of life, communities are not only seen as economic stimulators, but also as ecological regulators, which play an essential role in achieving sustainability. The selection of sustainability criteria is a key factor affecting the performance of Sustainable Urban Drainage Systems (SUDS). As the number of the sustainability criteria is often large and are not necessarily expressed in a common metric, sustainability evaluation can accordingly be formulated as a Multi-criteria Decision Analysis (MCDA) (Zhang et al., 2016).

1.4.3 Analytic Hierarchy Process (AHP)

Management problems are complex, which means that they are often described and defined in a too general way. Reduction of this complexity requires not only special knowledge, but also analytical skills supported by the right methodology. One concept that assists in the analysis of the complexity of management problems is the Analytic Hierarchy Process (AHP). The AHP, created by Saaty in 1980, is one of the suggestions for solutions concerning the construction and application of multi-criteria evaluation systems. The AHP can be defined as a process of hierarchizing a system as shown in Figure 1.2 in order to carry out a wide-ranging evaluation and a final selection of one of the alternative solutions to a particular problem. Its main focus is the measurement through pairwise comparisons and relies on the judgments of experts to derive priority scales. It is these scales that measure intangibles in relative terms.

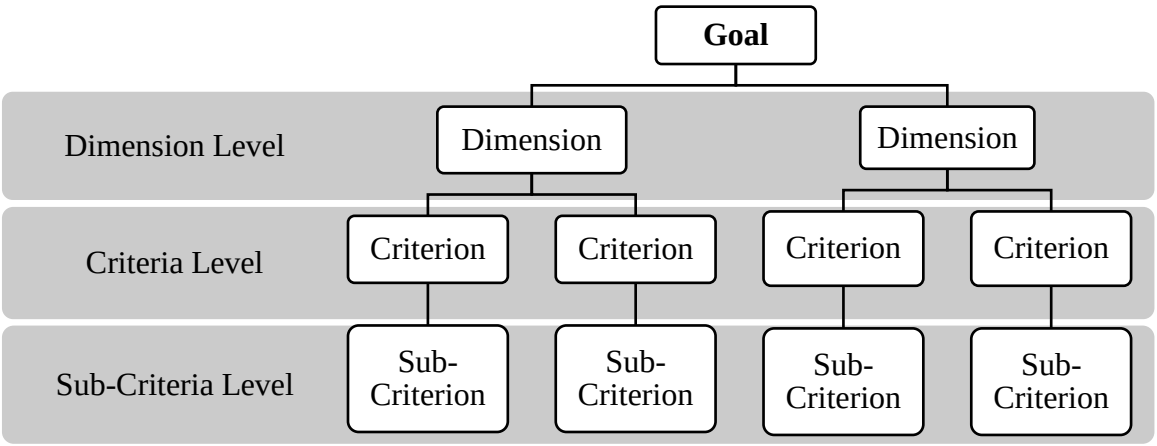

Figure 1.2: Generic Three Level Hierarchy Structure (Source: Zhang et al., 2016)

The comparisons are made using a scale of absolute judgments that represent how much more one element dominates another with respect to a given attribute (Saaty, 2008). For the most part, implementing the AHP method consists of a two-phase approach. In the first phase, the hierarchy structure of the system is prepared. As for the second phase, individual elements are evaluated and the consistency of the evaluation is checked. The evaluation works by comparing all pairs of elements at a given level from the point of view of each element located a level higher in the previously constructed hierarchical structure.

In order to quantify it, Saaty (2008) proposed a comparison scale, which relates the linguistic term to a numerical value. Table 1.2 summarizes these values. The result of the comparisons is a set of matrices, which form the basis for the final evaluation of the system after normalization and examination of consistency (Cabala, 2010).

Table 1.2: The fundamental scale of absolute numbers (after Saaty, 2008)

Intensity of Importance	Definition	Explanation
1	Equally Important	Two activities contribute equally to the objective
2	Weak or slight	
3	Slightly More Important	Experience and judgment slightly favor one activity over another
4	Slightly More Plus	
5	More Important	Experience and judgment strongly favors one activity over another
6	More Plus	
7	Much More Important	An activity is favored very strongly over another; its dominance demonstrated in practice
8	Very, very strong	
9	Absolutely More Important	The evidence favoring one activity over another is of the highest possible order of affirmation
Reciprocals of above	If activity *i* has one of the above non-zero numbers assigned to it when compared with activity *j*, then *j* has the reciprocal value when compared with *i*.	A reasonable assumption

1.4.3.1 AHP Steps (After Saaty, 2008)

1. Define the problem and determine the kind of knowledge sought.

2. Structure the decision hierarchy from the top with the goal of the decision, then the objectives from a broad perspective, through the intermediate levels (criteria on which subsequent elements depend) to the lowest level (which usually is a set of the alternatives).

3. Construct a set of pairwise comparison matrices. Each element in an upper level is used to compare the elements in the level immediately below with respect to it.

4. Use the priorities obtained from the comparisons to weigh the priorities in the level immediately below. Do this for every element. Then for each element in the level below add its weighed values and obtain its overall or global priority. Continue this process of weighing and adding until the final priorities of the alternatives in the bottom most level are obtained.

1.4.4 Glass

As of 2014, recycling in Puerto Rico represented only a 14%. In 1992, the Authority for Solid Waste in Puerto Rico (ADS, for its acronym in Spanish), established the implementation and development of cost effective and environmentally friendly strategies to reduce the volume of solid wastes (ADS, 2014). By 2012, around 610 tons of glass were recovered for recycling or manufacturing and exported nearly 750 tons. Being non-biodegradable in nature, glass disposal at landfills has environmental impacts and also could be expensive (Islam et al., 2017). The amount of waste glass is gradually increased over the recent years due to an ever growing used of glass products. Most of waste glass that is produced is dumped into landfill sites, roadways or illegal dumping areas In search for a new way to reduce the costs of disposal and the environmental impacts of glass, the use of glass as partial replacement of cement in the concrete industry has been studied. Milling of glass to micro-meter scale particle, can bring major energy, environmental and economic benefit when cement is partially replaced with milled waste glass for production of concrete (Islam et al., 2017)

1.4.4.1 Alkali-Silica reactions

Due to the presence of amorphous silica in glass and the alkaline nature of glass, the idea of using glass in concrete has traditionally given rise to concerns regarding the deleterious alkali-silica reactions (ASR) between the highly alkaline pore solution of cement paste and glass. It has been reported that the chemistry of ASR is similar to that of a pozzolanic reaction. The different effect of ASR versus the pozzolanic reaction in concrete arises mainly from the difference in particle size of the siliceous material (finer for pozzolanic and coarser for ASR). In a pozzolanic reaction, the alkali-silicate gel is formed in an environment rich in Ca^{2+} and except in a narrow zone close to the reacting surface, it is quickly converted into calcium silicate hydrate (C-S-H). On the contrary, in ASR it is formed in an environment that is poor in Ca^{2+}, and massive outflows of gel may result. The cement paste cannot supply Ca^{2+} fast enough to prevent much of this gel from persisting for long periods. Milling glass to powder size (similar to cement size) increases the surface area that is available for reaction in an environment where much calcium is still available in the solution. (Nassar et al., 2012)

1.4.5 Fly Ash

Fly Ash (FA) has been researched as a solution to reduce the CO_2 emissions of the cement industry. FA is also a waste, which generates from pulverized coal used on thermal power plants (Sahoo et al., 2016). In Puerto Rico, the only coal-based power plant, located in the municipality of Guayama, generates around 454 megavolts, which represents approximately 15% of the electricity consumed in the country (AES Puerto Rico, 2016). A significant portion of the production of the fly ash ends up at landfills, resulting in massive storage piles, latent environmental problems and distress in local communities (Blissett et al., 2012). Even though the compressive strength is reduced with the increment of fly ash content in concrete, due to the pozzolanic activity of fly ash, its compressive strength increases in the later stages of curing (i.e. 28 days) (Saha, 2017). Almusallam (1995) also studied the mechanical characteristics of hardened FA concrete by replacing cement content with FA and concluded that inclusion of FA results in higher compressive strength on later ages. The slow reactivity and lesser surface area of the FA are the reason of slower compressive strength gain. As for the glass, researches show that 15% to 20% of cement replaced with milled glass powder provides a compressive strength exceeding those of a control concrete (Islam et al., 2017).

1.4.6 Response Surface Methodology (RSM)

Due to a wide range of variability of mechanical properties in concrete, it is usually necessary to carefully plan an experimental design method to obtain a feasible mixture of concrete assessing the impact of the aggregates present in the mixture on the mechanical behavior of the concrete (Mtarfi et al., 2017). Response Surface Methodology (RSM) is a collection of mathematical and statistical techniques useful for the modeling and analysis of problems in which a response of interest is influenced by several variables and the objective is to optimize this response (Montgomery, 2013). When referring to concrete, the variables considered in the experiment would be represented by the aggregates in the mixture while as for the response, it will be denoted by the mechanical properties that want to be studied such as compressive strength, tensile strength, permeability, etc. A variable also referred as a factor, will have levels. A factor is defined as a controllable variable that is believed to have an effect on the response and a level refers to an experimental setting at which a factor will be evaluated (Montgomery, 2013).

For the design of the experiment, central composite design (CCD) has been the most commonly used design method with RSM in statistically assessing the mathematical relationship between the independent variables and the responses (Mtarfi et al., 2017). Generally, the CCD consists of a 2^k factorial with axial (i.e. lowest and highest levels) and center runs (Montgomery, 2013). Figure 1.3 shows a typical representation of a 2^k factorial design.

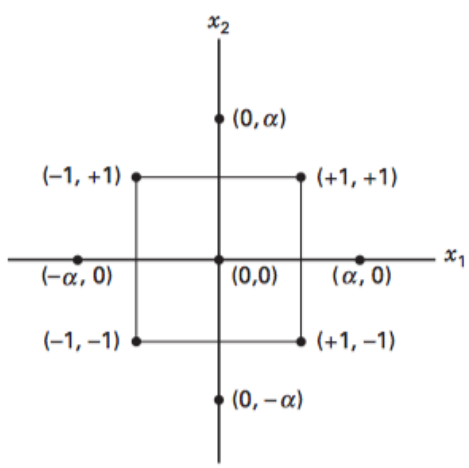

Figure 1.3: CCD 2^k factorial design

Moreover, statistically designed mixture experiments are quite useful in identifying the best combination of factors for achievement of optimized properties of concrete mixture. Factorial design, in which 'q' mixture components are reduced to q-1 independent factors by taking ratio of two components and the significance of each component and model for concrete could be determined using Analysis of Variance (ANOVA). The advantage of using ANOVA technique is that it allows the simultaneous study of the effect of all the parameters by carrying out this single analysis (Mukharjee et al., 2014). Understanding the effects of the aggregates on the mechanical properties of the concrete allows manipulation of the levels of the studied factors to manufacture sustainable mortars with durable properties (Mtarfi et al., 2017).

1.4.7 Pervious Concrete (PC)

A pervious concrete pavement system, as shown in Figure 1.4, is a combination of elements including pervious concrete, a base course of clean stone, and filter fabric or geotextile. Pervious concrete is a material typically produced with a conventional quantity of cementitious material, low water content, little or no sand, a relatively small, uniformly-sized coarse aggregate, and commonly used admixtures and air entraining agents. It generally has a relatively permeability of 3.5 gal/ft^2/min and a porosity of 15 to 25%. Pervious concrete can be a BMP used to mitigate problems associated with surface runoff through several mechanisms, such as capturing the first surface runoff, create short term storage detention of rainfall and also reduce the heat island effect (Leming et al., 2007).

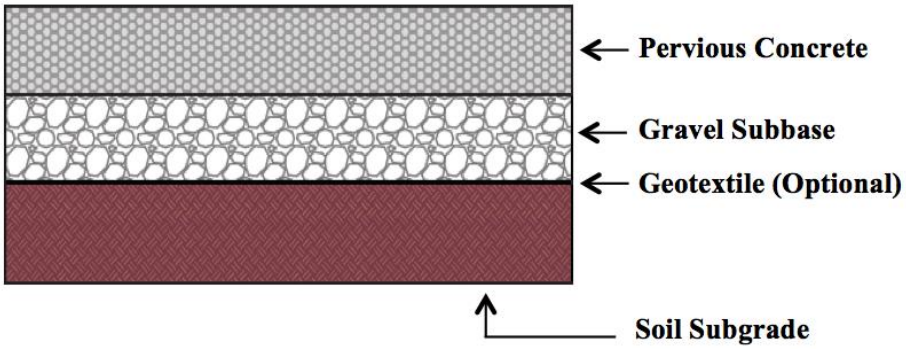

Figure 1.4: Typical cross section of a pervious concrete pavement system

1.4.8 Pervious Concrete Pavement as a Retention Structure

Pervious concrete pavement systems are often designed as retention structures. A significant advantage of pervious concrete pavement systems is the ability to park on the "pond," providing a multi-use facility with many additional advantages. Pervious concrete pavement systems provide a significant and unique value by simultaneously improving water quality, helping mitigate flooding, and returning the surface area to commercially productive use. The total storage capacity of the pervious concrete pavement system includes the capacity of the pervious concrete pavement, plus that of any base course used, and may be increased with optional storage features such as curbs, underground tanks and ground improvements (i.e. stone columns). The amount of runoff captured should also include the amount of water, which leaves the system by infiltration into the underlying soil. All of the voids in the pervious concrete will not be filled in service because some may be disconnected, some may be difficult to fill, and air may be difficult to expel from others. Therefore it is better to make reference to the porosity of the pervious concrete. The total storage capacity calculations will depend on the percentages of porosity for the pervious concrete layer and the aggregate base course. In fact, the total storage capacity will also depend on the system's slope (Leming et al., 2007).

2 MULTI-CRITERIA DECISION ANALYSIS (MCDA) APPLICATION ON SUSTAINABILITY

2.1 ABSTRACT

A sustainability assessment was done throughout the UPRM Campus to identify the critical areas in need of a pervious concrete pavement, equipped with a subsurface water retention structure. In order to carry out an objective evaluation of the areas, the MCDA was performed in conjunction with the AHP approach. The AHP approach consisted on a two-phase process in which the three sustainability categories: social, economic and environmental were ranked based on the different criteria that fell under each of them. To accomplish this goal, a group of ten experts were requested to fill out a questionnaire comparing the different evaluated criteria. A total of seven criteria were chosen: Impact on Daily Activities, Safety, Infrastructure Condition, Construction Costs, Stormwater Drainage System nearby, Topography and Surface Condition. Based on the experts, the criteria with the highest weight was Impact on Daily Activities with a value of 0.251, whereas the lowest was if there was any stormwater drainage system nearby with a value of 0.069. After weighting all of the criteria under each sustainability category, the category with the highest value was the social sustainability with a weighted value of 0.581. Additionally, after the on site assessment of the campus, there were seven critical areas identified. These were Las Palmas Avenue, Faculty Building, Physics Building, Mangual/Terrace, Nursing Building, Day Care Center and José de Diego Building. The assessment of these areas, using these criteria revealed that the ones in most need of a pervious concrete system were the Mangual/Terrace and Faculty Building with overall ranked values of 4.1 and 4.0, respectively.

2.2 METHODOLOGY

2.2.1 Design of the AHP Approach

The selection of sustainability criteria is a key factor affecting the performance of the UPRM campus sustainability. The different criteria were selected from the impacts and contributions the implementation of pervious concrete as a subsurface stormwater retention structure would partake. Figure 2.1 illustrates the proposed hierarchy structure to achieve an objective assessment for sustainability evaluation of each specific site. It is a two level hierarchy, in which the main goal is represented by the site identification, social, economic and environmental sustainability are the level one dimension while the level two is represented by the criteria specific for each dimension.

2.2.2 Hierarchy Structure

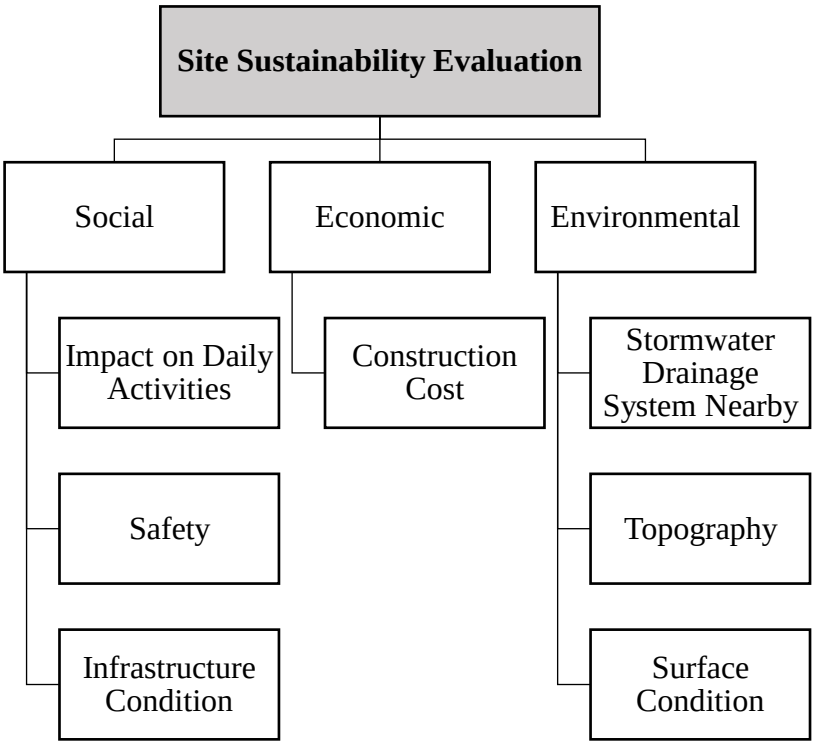

Figure 2.1: UPRM Site Evaluation Hierarchy Structure

2.2.3 Weighting of the hierarchical structure

A group of 10 experts was requested to give their assessment regarding the relative importance for each specific criterion. The group of experts was a representative from all related sectors such as engineering, surveying, architecture, and environmental health and safety with over 20 years of experience in their respective fields to give a balanced view on the topic. In order to perform the judging a questionnaire was done in which the expert provided a unique value for a set of comparison criteria. Simultaneously, the expert was also provided with a brief description of the research and an explanation for each of the criteria. A brief example of the questions was as follows:

"How important is criteria CX compared to criteria CY? To answer this question please used the information provided below and fill out corresponding values in the table."

Criteria:

C1. **Impact on daily activities** - The effect on people's normal daily living (i.e., how pervious concrete could improve people's functional mobility around campus)

C2. **Safety** - Refers to how pervious concrete would help manage and reduce potential risks to human life.

C3. **Infrastructure Condition** – The aesthetics of the site.

C4. **Construction Cost** – The expenses of implementing pervious concrete.

C5. **Stormwater drainage system nearby** – The effect of having a stormwater drainage system near the site. (Note: This would be beneficial since the pervious concrete system could potentially be connected to the existing system.)

C6. **Topography** – Does the site have a difference in elevation? Is the terrain flat or does it have a slope? Is the terrain irregular? (Note: The best condition is to have a flat surface.)

C7. **Surface Condition** – The % of green/pervious areas vs. % of impervious surfaces on site.

After the experts submit their individual judgments, the values for each pair comparison were transformed into a new scale, known as the fuzzy triangular scale. Ayhan (2013) detailed a series of steps due to the fact that the basic AHP does not include vagueness for personal

judgments. Table 2.1 illustrates the Saaty scale values, the linguistic terms and the corresponding triangular fuzzy scale.

Table 2.1: Linguistic terms and the corresponding triangular fuzzy numbers

Saaty Scale	Definition	Triangular Fuzzy Scale	Triangular Fuzzy Reciprocal
1	Equally Important	(1,1,1)	(1, 1, 1)
2	Weak or slight	(1,2,3)	(1/3, 1/2, 1)
3	Slightly More Important	(2,3,4)	(1/4, 1/3, 1/2)
4	Slightly More Plus	(3,4,5)	(1/5, 1/4, 1/3)
5	More Important	(4,5,6)	(1/6, 1/5, 1/4)
6	More Plus	(5,6,7)	(1/7, 1/6, 1/5)
7	Much More Important	(6,7,8)	(1/8, 1/7, 1/6)
8	Very, very strong	(7,8,9)	(1/9, 1/8, 1/7)
9	Absolutely More Important	(9,9,9)	(1/9, 1/9, 1/9)

Next step after the transformation was the construction of the pair comparison matrix. Because there are 10 experts, preferences of each were averaged and calculated.

$$\widetilde{\boldsymbol{A}}^{\boldsymbol{K}} = \begin{bmatrix} \widetilde{\boldsymbol{d}_{11}}^{\boldsymbol{k}} & \widetilde{\boldsymbol{d}_{12}}^{\boldsymbol{k}} & \cdots & \widetilde{\boldsymbol{d}_{1n}}^{\boldsymbol{k}} \\ \widetilde{\boldsymbol{d}_{21}}^{\boldsymbol{k}} & \cdots & \cdots & \widetilde{\boldsymbol{d}_{2n}}^{\boldsymbol{k}} \\ \cdots & \cdots & \cdots & \cdots \\ \widetilde{\boldsymbol{d}_{n1}}^{\boldsymbol{k}} & \widetilde{\boldsymbol{d}_{n2}}^{\boldsymbol{k}} & \cdots & \widetilde{\boldsymbol{d}_{nn}}^{\boldsymbol{k}} \end{bmatrix}$$

Where $\widetilde{\boldsymbol{A}}^{\boldsymbol{K}}$ indicates the pair comparison matrix, kth indicates a respective expert, $\widetilde{\boldsymbol{d}_{nn}}$ specifies the preference the kth expert makes of a specific criterion over the other criterion and the tilde represents triangular fuzzy scale. Because there was more than one expert, the preferences were averaged as shown in Equation 2.1:

$$\widetilde{d_{ij}} = \frac{\sum_{k=1}^{K} \widetilde{d_{ij}}^{k}}{K} \tag{2.1}$$

Where $\widetilde{d_{ij}}$ represents the kth expert's preference of criterion ith over jth.

The resulting pairwise comparison matrix was updated as follows:

$$\tilde{A} = \left[\begin{pmatrix} \widetilde{\boldsymbol{d_{11}}} & \cdots & \widetilde{\boldsymbol{d_{1n}}} \\ \vdots & \ddots & \vdots \\ \widetilde{\boldsymbol{d_{n1}}} & \cdots & \widetilde{\boldsymbol{d_{nn}}} \end{pmatrix}\right]$$

Afterwards, the geometric mean for the fuzzy values was calculated using Equation 2.2:

$$\widetilde{r_i} = \left(\prod_{j=1}^{n} \widetilde{d_{ij}}\right)^{1/n}, \qquad i = 1, 2, \dots n \tag{2.2}$$

Where, $\widetilde{r_i}$ is the geometric mean, and Π is the vector summation of each triangular value.

The fuzzy weight for criterion (i) was calculated, multiplying each $\widetilde{r_i}$ with the reverse vector as shown in Equation 2.3:

$$\widetilde{w_i} = \widetilde{r_i} \otimes (\widetilde{r_1} \oplus \widetilde{r_2} \oplus \dots \oplus \widetilde{r_n})^{-1} = (lw_i, mw_i, u_i) \tag{2.3}$$

In order to de-fuzzied the triangular numbers $\widetilde{w_i}$, the center or area method was applied as illustrated in Equation 2.4:

$$M_i = \frac{lw_i + mw_i + uw_i}{3} \tag{2.4}$$

The final step required the normalization of M_i, which was calculated using Equation 2.5 as follows:

$$N_i = \frac{M_i}{\sum_{i=1}^{n} M_i} \tag{2.5}$$

The resultant normalized values from each criteria were then be weighted to obtain an overall value for each of the three dimensions.

2.2.4 Reconnaissance and Site Identification

As part of the reconnaissance phase for the eligible sites, several actions were put to practice in order to gather as much data and information as possible. All sites were visited during different weather conditions to better visualize and compare the degree of impact that each of the sites undergo when a rainfall events occurs versus when the surface is in dry conditions. The reconnaissance included:

- **Photographic log -** The log allowed saving and retrieving the site visit data
- **Opinion Poll** – It is important to gather the opinion of the students and employees that make use of the site on a daily basis
- **Assessment** – In order to select one overall alternative from the sites, each of them was evaluated under the previously mentioned criteria and was given a ranking score from 1 to 5, with 5 being the worst. The site with the highest score was the one in the most need of the pervious concrete subsurface retention structure.

2.2.5 Area of Study

A representation of the area on where the empirical study on the UPRM campus sustainability will take place is illustrated in Figure 2.2.

Figure 2.2: UPRM Campus (Source: Google Earth, 2017)

2.2.6 Ranking within the Criteria

In order to carry out the assessment for the critical sites in need of the implementation of pervious concrete pavement, each evaluated criteria was received a weighted value between (1-5) according to its positive or negative impact. The criteria as mentioned and discussed earlier were:

- ***Impact on daily activities***
  - Low = 1
  - Average = 3
  - High = 5
- ***Safety***
  - Safe = 1
  - Not Safe = 5
- ***Infrastructure Condition***
  - Good = 1
  - Average = 3
  - Bad = 5
- ***Construction Costs***
  - Low = 1
  - Average = 3
  - High = 5
- ***Stormwater drainage system nearby***
  - Yes = 1
  - No = 5
- ***Topography***
  - Flat = 1
  - Slope = 5
- ***Surface Condition***
  - Green Area = 1
  - Green Area and Asphalt/Concrete = 3
  - Asphalt/Concrete = 5

After the evaluation of each site and the assignment of an individual value for each criterion, a weighted sum for all values was done to obtain a total value for the site. After a final value had been reached, this value was multiplied by the value obtain from the experts questionnaire, which generated a final ranking for each of the evaluated sites. The sites with the highest ranking were the ones that require urgent attention. Subsequently, those with the lowest values had the minor priority. Nevertheless, the areas with the lowest values weren't to be at all ignored, and would require thorough attention.

2.2.7 Selection of critical Sites

For the selection of the most critical sites on campus, a thorough assessment was conducted during rainy conditions to help identify areas prone to flash flooding. The results of the assessment demonstrated that seven sites were the most susceptible to flood or ponding as shown in Figure 2.3. These were: Las Palmas Avenue (Figure 2.4), Faculty Building (Figure 2.5), Physics Building (Figure 2.6), Nursing Building (Figure 2.7), Mangual Coliseum/Terrace (Figure 2.8), Day Care Center (Figure 2.9) and José de Diego Building (Figure 2.10). After completing the identification, each site was visited again during sunny weather conditions for their evaluation against each criterion. Table 2.2 shows the ranking value assigned on each criterion for the identified critical sites.

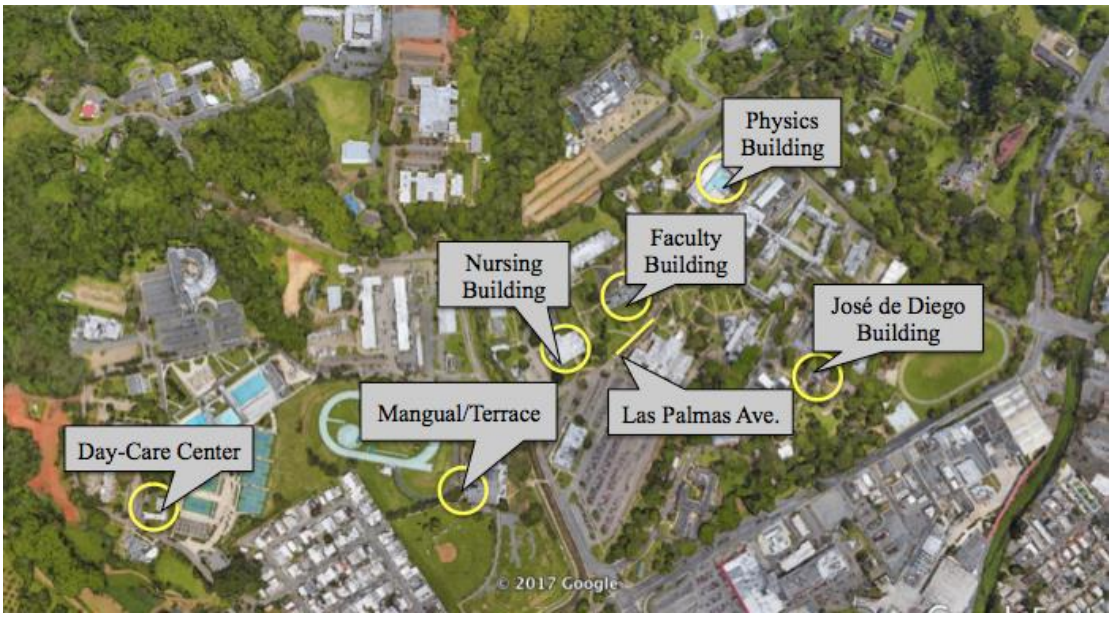

Figure 2.3:Identified critical sites

Figure 2.4: Las Palmas Avenue

Figure 2.5: Faculty Building

Figure 2.6: Physics Building

Figure 2.7: Nursing Building

Figure 2.8: Mangual/Terrace

Figure 2.9: Day care Center

Figure 2.10: José de Diego Building

Table 2.2: Ranked Values for the Assessed Sites

Site	Impact on Daily Activities	Safety	Infrastructure Condition	Construction Costs	Stormwater system nearby	Topography	Surface Condition
Las Palmas Avenue	5	5	1	3	1	1	3
Faculty Building	5	5	5	3	1	1	5
Physics Building	5	3	1	1	1	1	1
Nursing Building	5	5	1	3	5	1	1
Mangual/Terrace	5	5	3	3	5	5	3
Day Care Center	1	3	1	1	1	1	5
José de Diego Building	1	1	1	1	1	5	3

2.3 RESULTS AND DISCUSSION

2.3.1 AHP

The data contained in Table 2.3 was processed by the fuzzy AHP methodology previously described in Section 2.2.3 to obtain the set of relative weights of each of the components of the decision-making tree represented in Figure 2.1. Then, the previously discussed procedure was developed to obtain an average value on each of the comparison criteria as shown in Table 2.4. Accordingly, the fuzzy value for each comparison was attained and the pairwise comparison matrix was built as illustrated in Table 2.5. Afterwards, the fuzzy weights were calculated as shown in Table 2.6. The resultant defuzzied and normalized values for each criterion were calculated by applying Equation 1.4 and Equation 1.5 were the final results are shown in Table 2.7. Based on the results, the criterion with the highest value was the impact on daily activities, whereas the criterion with the lowest value was if there was a stormwater drainage system nearby the site.

Table 2.3: Expert's judgment regarding each of the criteria

Pairwise Comparison	Expert Number									
	1	2	3	4	5	6	7	8	9	10
C1 vs. C2	EI	MMI	SMI	EI	EI	EI	EI	MMI	MMI	EI
C1 vs. C3	AMI	MI	EI	MI	SMI	W	AMI	SMI	MMI	MI
C1 vs. C4	AMI	EI	EI	SMI	MI	SMI	MI	EI	MI	EI
C1 vs. C5	EI	MMI	SMI	EI	MMI	EI	W	EI	MI	SMI
C1 vs. C6	AMI	EI	MI	AMI	SMI	EI	MI	SMI	SMI	MI
C1 vs. C7	EI	EI	EI	MMI	EI	EI	EI	MI	MMI	MI
C2 vs. C3	AMI	EI	EI	AMI	EI	EI	AMI	AMI	MMI	AMI
C2 vs. C4	AMI	EI	EI	MMI	EI	AMI	AMI	MI	MI	MMI
C2 vs. C5	AMI	EI	SMI	SMI	EI	SMI	MMI	MI	SMI	MMI
C2 vs. C6	AMI	EI	SMI	EI	MMI	SMI	MMI	MI	SMI	MMI
C2 vs. C7	AMI	AMI	EI	SMI	MMI	SMI	MI	MI	MMI	MI
C3 vs. C4	EI	MI	EI	EI	MI	SMI	EI	EI	AMI	EI
C3 vs. C5	MI	EI	SMI	EI	EI	SMP	EI	SMI	MMI	EI
C3 vs. C6	EI	EI	SMI	EI	SMI	W	EI	SMI	MMI	EI
C3 vs. C7	MMI	EI	EI	EI	EI	EI	EI	SMI	AMI	EI
C4 vs. C5	EI	AMI	EI	SMI	EI	SMI	MI	EI	MI	MI
C4 vs. C6	SMI	EI	EI	EI	EI	W	MMI	SMI	MMI	MI
C4 vs. C7	MI	MMI	EI	EI	SMI	W	MI	EI	MMI	MMI
C5 vs. C6	MMI	AMI	EI	MMI	SMI	EI	MMI	SMI	MMI	EI
C5 vs. C7	MMI	MI	EI	MI	MI	EI	MI	SMI	MI	EI
C6 vs. C7	MMI	EI	EI	AMI	MMI	EI	EI	EI	MI	EI

Table 2.4: Expert's judgment in the Saaty scale with the respective averaged fuzzy value

Pairwise Comparison	Expert Number											
	1	2	3	4	5	6	7	8	9	10	Average	Fuzzy Value
C1 vs. C2	1	7	3	1	1	1	1	7	7	1	3	(2, 3, 4)
C1 vs. C3	9	5	1	5	3	2	9	3	7	5	5	(4, 5, 6)
C1 vs. C4	9	1	1	3	5	3	5	1	5	1	3	(2, 3, 4)
C1 vs. C5	1	7	3	1	7	1	2	1	5	3	3	(2, 3, 4)
C1 vs. C6	9	1	5	9	3	1	5	3	3	5	4	(3, 4, 5)
C1 vs. C7	1	1	1	7	1	1	1	5	7	5	3	(2, 3, 4)
C2 vs. C3	9	1	1	9	5	1	9	9	7	9	6	(5, 6, 7)
C2 vs. C4	9	1	1	7	5	9	9	5	5	7	6	(5, 6, 7)
C2 vs. C5	9	1	3	3	5	3	7	5	3	7	5	(4, 5, 6)
C2 vs. C6	9	1	3	1	7	3	7	5	3	7	5	(4, 5, 6)
C2 vs. C7	9	9	1	3	7	3	5	5	7	5	5	(4, 5, 6)
C3 vs. C4	1	5	1	1	5	3	1	1	9	1	3	(2, 3, 4)
C3 vs. C5	5	1	3	1	1	4	1	3	7	1	3	(2, 3, 4)
C3 vs. C6	1	1	3	1	2	2	1	3	7	1	2	(1, 2, 3)
C3 vs. C7	7	1	1	1	1	1	1	3	9	1	3	(2, 3, 4)
C4 vs. C5	1	9	1	3	1	3	5	1	5	5	3	(2, 3, 4)
C4 vs. C6	3	1	1	1	1	2	7	3	7	5	3	(2, 3, 4)
C4 vs. C7	5	7	1	1	3	2	5	1	7	7	4	(3, 4, 5)
C5 vs. C6	7	9	1	7	3	1	7	3	7	1	5	(4, 5, 6)
C5 vs. C7	7	5	1	5	5	1	5	3	5	1	4	(3, 4, 5)
C6 vs. C7	7	1	1	9	7	1	1	1	5	1	3	(2, 3, 4)

Table 2.5: Fuzzy Comparison Matrix

	C1	C2	C3	C4	C5	C6	C7
C1	(1, 1, 1)	(2, 3, 4)	(4, 5, 6)	(2, 3, 4)	(2, 3, 4)	(1/5, 1/4, 1/3)	(2, 3, 4)
C2	(1/4, 1/3, 1/2)	(1, 1, 1)	(1/7, 1/6, 1/5)	(1/7, 1/6, 1/5)	(4, 5, 6)	(4, 5, 6)	(4, 5, 6)
C3	(1/6, 1/5, 1/4)	(5, 6, 7)	(1, 1, 1)	(2, 3, 4)	(2, 3, 4)	(1/3, 1/2, 1)	(2, 3, 4)
C4	(1/4, 1/3, 1/2)	(5, 6, 7)	(1/4, 1/3, 1/2)	(1, 1, 1)	(2, 3, 4)	(2, 3, 4)	(1/5, 1/4, 1/3)
C5	(1/4, 1/3, 1/2)	(1/6, 1/5, 1/4)	(1/4, 1/3, 1/2)	(1/4, 1/3, 1/2)	(1, 1, 1)	(4, 5, 6)	(1/5, 1/4, 1/3)
C6	(3, 4, 5)	(1/6, 1/5, 1/4)	(1, 2, 3)	(1/4, 1/3, 1/2)	(1/6, 1/5, 1/4)	(1, 1, 1)	(2, 3, 4)
C7	(1/4, 1/3, 1/2)	(1/6, 1/5, 1/4)	(1/4, 1/3, 1/2)	(3, 4, 5)	(3, 4, 5)	(1/4, 1/3, 1/2)	(1, 1, 1)

Table 2.6: Calculated fuzzy weights for each criteria

Criteria	$\widetilde{w_i}$		
1	0.148	0.254	0.416
2	0.087	0.134	0.210
3	0.115	0.196	0.334
4	0.084	0.139	0.235
5	0.042	0.067	0.115
6	0.065	0.112	0.186
7	0.060	0.097	0.165

Table 2.7: Defuzzied and normalized values for the criteria

Criteria	M_i	N_i
1	0.273	0.251
2	0.144	0.132
3	0.215	0.198
4	0.153	0.140
5	0.075	0.069
6	0.121	0.111
7	0.107	0.099

Based on the experts' questionnaire results and after obtaining the normalized values for the criteria, the final hierarchy structure for the objective assessment of sustainability was developed. Social sustainability had the most weight with a value of 0.581. Secondly, was environmental sustainability with a value of 0.279 and the last was the economic sustainability with a value of 0.140. Figure 2.11 shows the hierarchy structure with the calculated values for the criteria and the weighted total values for each category of sustainability.

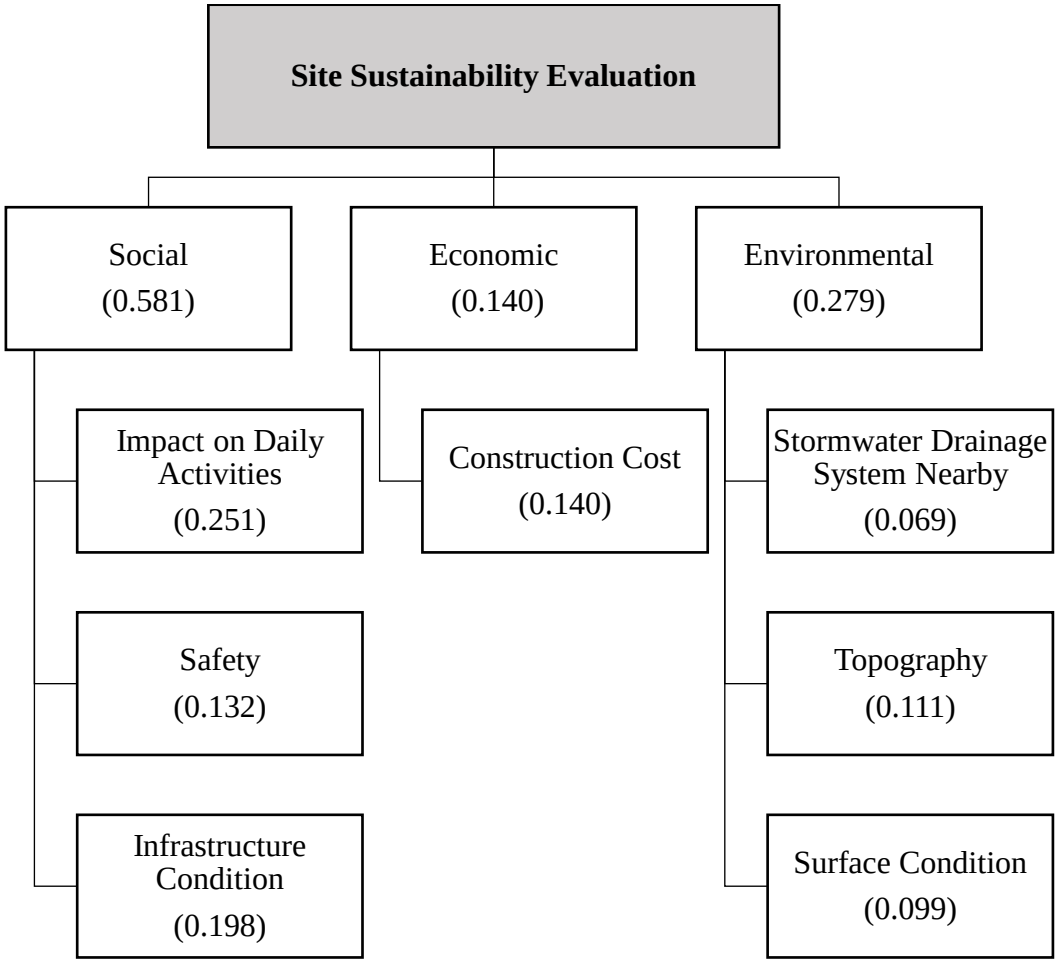

Figure 2.11: Hierarchy structure with measured values for the evaluated criteria

2.3.2 Site Identification Ranking

To calculate a final ranking, each criteria value is multiplied by the value assigned during the evaluation of the sites. Results indicated that the sites with the highest values and correspondingly in most need of pervious concrete implementation, were Mangual/Terrace and Faculty Building with a total ranking of 4.1 and 4.0, respectively. Figure 2.12 shows the overall ranking values of all the assessed sites.

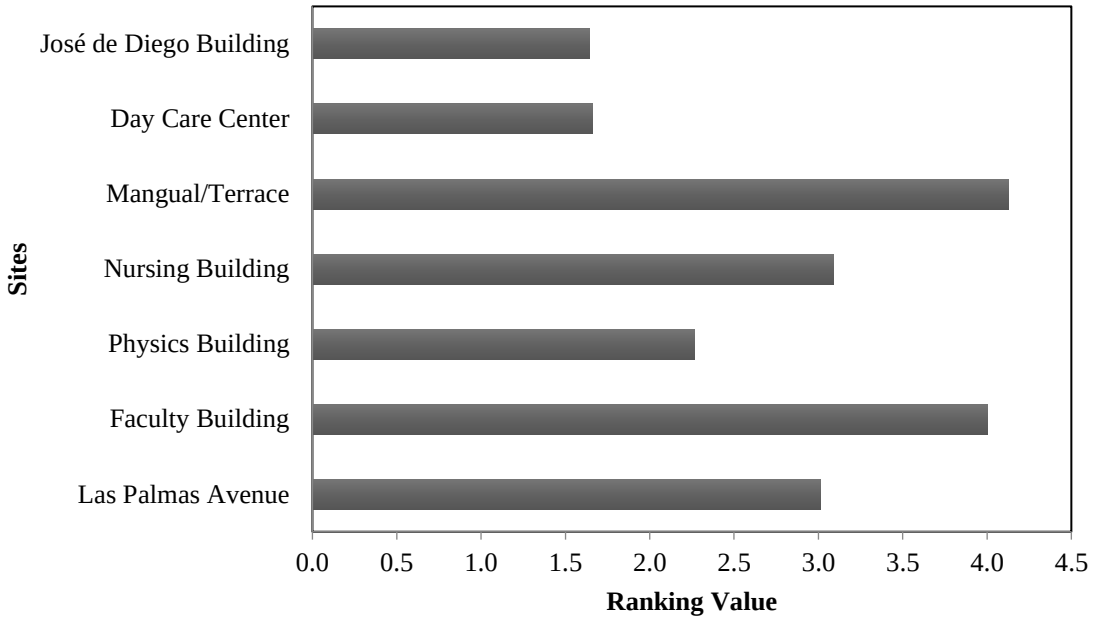

Figure 2.12: Ranked values for the assessed sites

2.4 CHAPTER CONCLUSIONS

After the application of the MCDA with the AHP approach on campus sustainability, the following conclusions can be drawn:

- Impact on daily activities resulted to be the criterion with the highest value and stormwater drainage system nearby was the lowest with 0.251 and 0.069, respectively.
- Social Sustainability weighted the most out of the three evaluated sustainability categories with an overall value of 0.581.
- The areas in most need of the implementation of a pervious concrete system were the Mangual/Terrace and Faculty Building with overall ranked values of 4.1 and 4.0, respectively.
- Results from the model showed the usefulness of the AHP that enabled to obtain an objective approach when implementing the MCDA.

3 OPTIMIZATION OF WASTE GLASS POWDER AND FLY ASH AS PARTIAL REPLACEMENT OF CEMENT IN MORTAR

3.1 ABSTRACT

The goal of this study was to attain an optimized mortar mixture incorporating glass and fly ash as partial replacement of cement. Given the lack of glass recycling and high quantities of fly ash that end up at landfills in P.R., their incorporation as construction materials was studied. As a result of the presence of silica in both glass and fly ash, a pozzolanic reaction is produced at later ages (i.e. 28 days) exhibiting higher compressive strength values than regular concrete. X-ray diffraction (XRD) and a hydrometer test were done to analyze the chemical composition of the glass and the particle size distribution respectively. XRD revealed an amorphous pattern on the glass while the hydrometer test results showed the cumulative measure for 50% of the particle size was 8 µm. The optimization of the mixture was made using RSM to get the highest possible compressive strength value, with a targeted spread percentage of 110%. A two-factor, two-level CCD was chosen to study the effects of glass-to-binder ratio (G/B) and fly ash-to-binder ratio (FA/B). At 28 days of curing, the compressive strength values ranged from 74 to 84.6 MPa while the spread percentage ranged from 86.1 to 119.3%. The compressive strength response was found to increase with a decrease in both G/B and FA/B. For the spread percentage response, there also needs to be a decrease in G/B and FA/B to obtain higher values. Nevertheless, the G/B range selected provided a good region for the desired spread percentage of 110%. The optimum values for a compressive strength of 83 MPa and 110 spread percentage were 7.25% G/B and 14.30% FA/B. Validation results indicated an 11% difference between the expected compressive strength value and the measured one. Even though it was not included in the optimization, a splitting tensile strength test was also done on mortar specimens at 28 days of curing. Results from the test exhibited a tensile strength of 13.6 MPa. In addition, the compressive strength was measured at 7 and 56 days with values of 53.8 and 88.9 MPa, respectively.

3.2 MATERIALS

As part of the mortar specimen, Portland Cement Type GU provided by Argos San Juan (previously known as Essroc Italcementi Group) and conforming to ASTM C150 was used. Fly Ash was obtained from AES Puerto Rico, which is a local coal-fueled power plant located in the municipality of Guayama. According to ASTM C618, the FA cannot be classified as either Class C or Class F due to its high content of SO_3 and Loss on Ignition (LOI), which surpass the maximum allowable of 5% and 6%, respectively. Table 3.1 shows the chemical properties for both the cement and fly ash. Waste milled glass with an average particle size of 8 μm was obtained through four phases as shown schematically in Figure 3.1. The first phase consisted of the recollection of local beer amber bottles. After their recollection, the second phase consisted of the removal of labels. In order to do so, the bottles were put inside a tank that was filled with lime ($Ca(OH)_2$)-saturated water and remained soaked for about 30 minutes. The third phase consisted in the sterilization of the bottles while as for the fourth phase the bottles were put inside a ball mill for approximately 4 hours at a rotational speed of 30 rpm in order to attain the desired particle size within the micrometer scale. 25 bottles were put in a stainless milling chamber in a volume of 0.03 m^3 in the presence of 300 stainless balls in a diameter of 2.54 cm. For admixture and conforming to ASTM C494, MasterMatrix VMA 362 viscosity-modifying admixture (VMA) provided by BASF was used.

Table 3.1: Chemical composition and physical characteristics of type GU of cement and fly ash

Compound	Cement Type GU (% wt.)	Fly Ash (% wt.)
SiO_2	19.7	30.8
Al_2O_3	4.9	9.9
Fe_2O_3	3.0	5.0
CaO	67.7	39.6
MgO	0.8	0.4
SO_3	2.7	11.4
Na_2O	-	0.9
K_2O	-	1.0
P_2O_5	-	0.1
TiO_2	-	0.5
Loss on Ignition (LOI)	7.8	7.6
Specific Gravity	3.1	2.55
Blaine (m^2/kg)	501	441
Fineness [a]	92.5	73.7

[a] Wet Sieve percentage passing the 45-μm (No. 325) sieve.

Figure 3.1: Process of milling glass bottles

3.2.1 Hydrometer Test

A hydrometer test was performed in accordance with ASTM D7928, which is used for size distribution for particles finer than the No.200 sieve (75 μm). Hydrometer analysis is based on Stokes law. According to this law, the velocity at which grains settles out of suspension, all other factors being equal, is dependent upon the shape, weight and size of the grain. In case of soil, it is assumed that the soil particles are spherical and have the same specific gravity. Therefore it can be said that in a soil water suspension, the coarser particles will settle more quickly than the finer ones (ASTM D7928). A 125 mL solution was prepared and a Type 152H Hydrometer was used for the test duration of 24 hr. as shown in Figure 3.2. The sample characteristics are listed in Table 3.2 whereas the hydrometer test results are shown in Table 3.3. Based on the test results, it was confirmed that the larger the particle size, the quicker it settles and vice versa. Figure 3.3 shows the granulometric curves for the glass powder and Portland cement (Ng et al., 2016). Based on the observation of the particle size distribution for glass powder and Portland cement, it is observed that the first one showed a lower size range distribution. Additionally, the cumulative measure D_{50} for the glass powder was analyzed and resulted in a particle size value of 8 μm.

Figure 3.2: Hydrometer Test

Table 3.2: Hydrometer test data

Characteristics	Value
Type of Hydrometer	152H
Prepared Solution	125ml
Weight of Dry Sample	48.93 g
Specific Gravity	2.8
Correction Factor, a	0.97
Representative Mass, W	50.00 g
Weight of Wet Representative Sample	15.00 g
Weight of Dry Representative Sample	14.68 g
Correction Factor for the Sample	0.97867 g

Table 3.3: Hydrometer test results

Time (min)	Reading, R (g/l)	Temperature (°C)	Percentage of fines	Effective Depth, L (cm)	Factor K	Particle Diameter (µm)
2	41	23.5	79.54	9.6	0.0125	30.10
5	32	23.5	62.08	11.1	0.0125	13.92
15	21.5	23.5	41.71	12.8	0.0125	5.35
30	15	23.5	29.1	13.8	0.0125	2.88
60	11	23	21.34	14.5	0.0126	1.52
250	8	23.5	15.52	15	0.0125	0.38
1440	7	23	13.58	15.2	0.0126	0.07

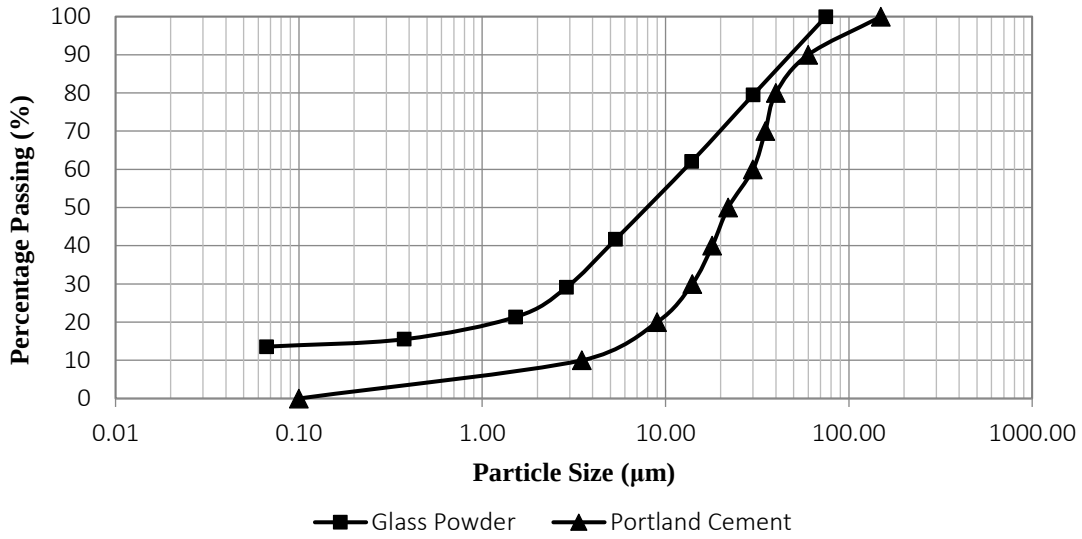

Figure 3.3: Granulometric curves comparison for glass powder and Portland cement (Ng et al., 2016) particle size distribution

3.2.1.1 Alkali-Silica Reaction

Using waste glass as coarse and fine aggregate in concrete can lead to expansions, due to the alkali-silica reaction (ASR). Nevertheless several researchers have found that glass powder less than 60 µm exhibited an increase in the pozzolanic reaction. They demonstrated that a smaller glass particle size led to a higher reactivity with lime, a higher compressive strength in concrete, and a lower expansion related to alkali-silica reaction (Kim et al., 2015). Based on the hydrometer test results the particle size range varied from 0.07 to 30.10 µm, thus revealing that an ASR expansion would not be expected in the mortar. Nassar et al. (2012) reported that for a particle size range between 0.4 and 50 µm there was no ASR expansion observed. Nassar concluded that the milling of waste glass to sub-micron particle size is key to benefit from its pozzolanic reaction. The high surface area of milled waste glass changes the kinetics of chemical reaction towards beneficial pozzolanic reaction utilizing the available alkalis before production of a potential ASR gel.

3.2.2 X-Ray Diffraction (XRD)

X-Ray Diffraction (XRD) was performed on the milled glass to quantify its chemical composition. Figure 3.4 shows the results from the test, which features the glass powder as an amorphous solid without any symmetry, which coincides with an issue released by the Clean Washington Center on recycled glass. The issue states that while SiO_2 is a primary ingredient in the manufacturing of bottle glass, when glass is formed, the crystalline structure is changed to an amorphous structure and the SiO_2 is no longer considered crystalline (Clean Washington Center, 2016). Nevertheless, Figure 3.5 depicts that although there was a lot of background noise, a specific percentage for chemicals present in the glass could not be determined but still showed presence of Silica (SiO_2), Alumina ($K_2Al_{24}O_{37}$), Potassium Vanadium Oxide (KVO_3) and Magnesium Cobalt Oxide ($MgCo_2O_4$).

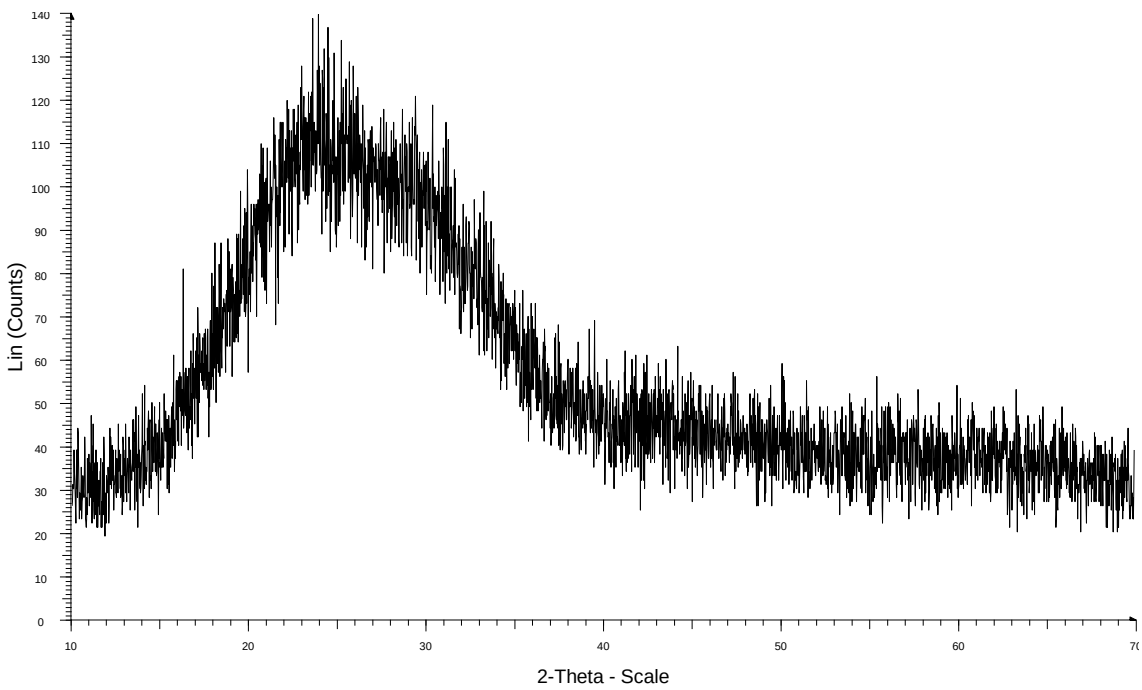

Figure 3.4: X-ray diffraction pattern of the glass powder

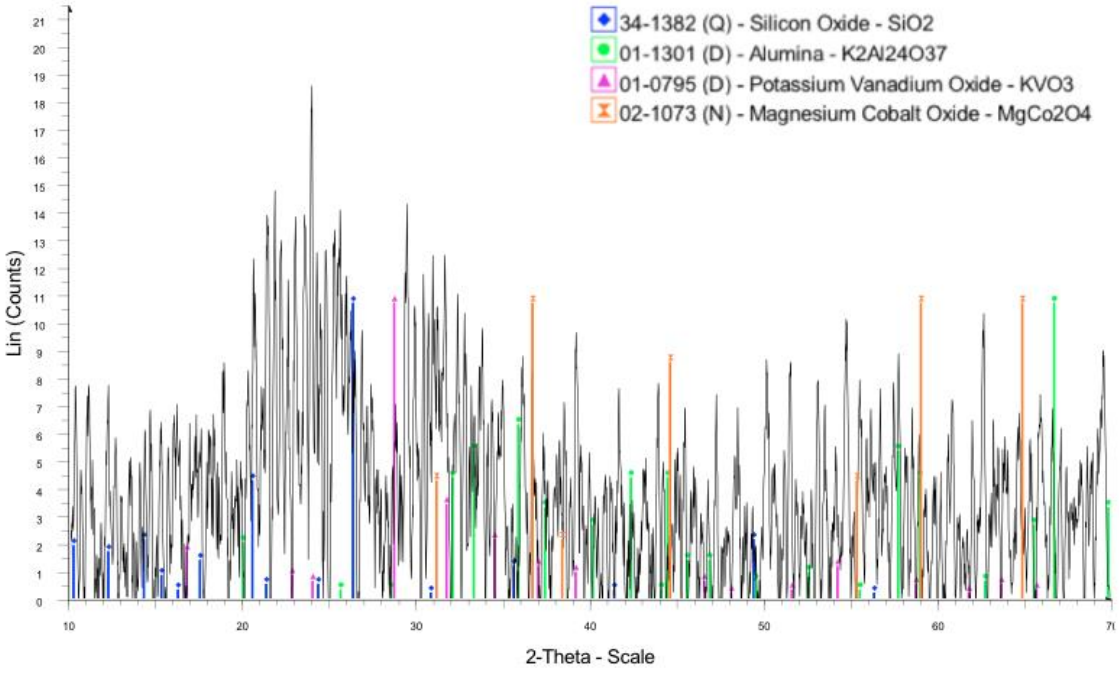

Figure 3.5: X-ray diffraction pattern with chemical composition

3.3 METHODOLOGY

3.3.1 Response Surface Methodology (RSM)

In this study, mortar specimens containing cement, glass and fly ash were made in triplicate in a 2^2 CCD. The two factors considered in the experimental design were glass-to-binder ratio (G/B) and fly ash-to-binder ratio (FA/B) with percentages ranging from 7.5% to 12.5% and 12.5% to 17.5%, respectively as shown in Table 3.4. In this specific design, upper and lower levels and boundaries are taken into consideration and are represented by the ±1 and ±α symbols. For this experiment, the binder (B) is defined as the total amount of Portland cement, glass (G) and fly ash (FA). A total of fourteen combination mixes were obtained from performing a Response Surface Methodology (RSM) which was utilized to optimize the mix design in order to achieve a time-dependent maximum compressive strength of cement pastes cured for 7, 28 and 56 days.

ANOVA was used to analyze the significance of the factors to the measured responses. A confidence of 95% was chosen, which means that factors resulting in p-values of 0.05 or less are statistically significant, thus are considered for the predicted regression model. Additionally, contour plots were interpreted to see how the response variable relates to the factors. The optimum mortar mix obtained from the optimizer tool was validated to test the accuracy of the model.

Table 3.4: Levels of the 2^2 factorial CCD design

Factors	Levels				
	-α	-1	0	+1	+α
Glass/Binder	5	7.5	10	12.5	15
Fly Ash/Binder	10	12.5	15	17.5	20

3.3.2 Specimen Design and Preparation

Fourteen mortar mixtures were prepared using a mechanical mixer in accordance to the ASTM C192 to examine the effects of FA/B and G/B on the workability, compressive strength and tensile strength in compliance with ASTM C1437, ASTM C39 and ASTM C496 respectively. All mixes were prepared using tap water and water-to-binder (w/b) ratio of 0.3. Even though it is a low w/b, compared to regular cement paste, it is important to mention that this paste will be used in a pc mixture design, which will be later discussed in Chapter 4. The w/b is an important consideration for obtaining desired strength void structure in pervious concrete. A high w/b reduces the adhesion of the paste to the aggregate and causes the paste to flow and fill the voids even when lightly compacted. A low w/b will prevent good mixing and an even distribution of binder paste, reducing the strength and durability of the concrete. Experience has shown that w/b in the range of 0.26 to 0.45 will provide the best aggregate coating and paste stability (ACI, 2010).

3.3.3 Compressive Strength and Tensile Strength

Cylindrical specimens (50mm x 100mm) for each mix were produced to test compressive strength. The samples were cured under limewater for 7 and 28 days and then tested. Each compressive strength value was obtained from the average value of three tests reported in MPa.

The tensile strength test was performed only on the optimized mix at 28 days of curing. The experimental results of the splitting tensile were evaluated and compared with empirical models pre-established in the literature, recommended by researchers or established by codes such as the one by the American Concrete Institute (ACI). Both the compressive and splitting tensile strength tests were performed using a 3000 kN Forney universal testing machine as illustrated in Figure 3.6. To provide a uniform load distribution, capping rubber pads (Gilson HM-362) were used.

Figure 3.6: Compressive Strength Test (Left) and Tensile Strength Test (Right)

3.3.4 Flow Test (Spread percentage)

Spread percentages of fresh binder pastes of the experimental designs were determined using a flow table in accordance with ASTM C1437. A conical mold with a bottom diameter of 10 cm was placed at the center of the flow table and was filled with fresh binder paste. Twenty tamps were applied after each filling layer to ensure uniformity in the mold. The remaining excess paste was cleaned out and the conical mold was removed. The flow table was then dropped 25 times in 15 seconds. An illustration of the procedure is depicted in Figure 3.7. The increase in base diameter was recorded and the spread percentage of the fresh binder paste was calculated.

Figure 3.7: Spread percentage test

3.4 RESULTS AND DISCUSSION

3.4.1 RSM Measured Responses

The testing for the spread percentage was done per run while as for the compressive strength of the 28-day cured specimen it was done in triplicate. For each compressive strength test run, the averages were calculated. Results indicated that the lowest value obtained was 74.0 MPa and the highest was 84.6 MPa. For a 28 days compressive strength, ASTM C150 recommends a minimum value of 28 MPa for Portland cement. When comparing the values achieved with a mortar composed of glass, fly ash and cement, it can be concluded that these were higher. For the spread percentage test, the values ranged from 86.1% up to 119.3%. Table 3.5 depicts the matrix for the design with the respective measured responses.

Table 3.5: Matrix of a 2^2 factorial CCD design and the averaged measured responses

Run	Independent Variables		Dependent Variables	
	G/B (% wt.)	FA/B (% wt.)	Spread (%)	Compressive Strength (MPa) 28 days
1	7.5	12.5	110.4	81.8
2	10	15	101.0	79.3
3	7.5	17.5	98.5	81.5
4	10	15	108.4	82.3
5	12.5	17.5	106.9	74.4
6	12.5	12.5	116.8	74.0
7	10	15	113.9	81.9
8	10	20	103.5	75.0
9	10	15	107.9	79.4
10	5	15	111.9	84.6
11	10	15	109.4	80.0
12	10	15	102.0	76.6
13	10	10	119.3	80.8
14	15	15	86.1	79.5

3.4.2 Statistical Model

The ANOVA for spread percentage and compressive strength is illustrated in Table 3.6. In order to validate the suitability of the model, residual plots and the lack of fit were evaluated. It should be noted that in order to improve the model's fit, a Box-Cox transformation was done. In practice, many experimenters select the form of the transformation by simply trying several alternatives and observing the effect of each transformation on the plot of residuals versus the predicted response. The transformation that produced the most satisfactory residual plot is then selected. Box-Cox Method allows the selection of a variance-stability transformation (Montgomery, 2013). The analysis from ANOVA depicts that for spread percentage, only FA/B was significant with a p-value of 0.021. On the contrary, for compressive strength, only G/B was significant with a p-value of 0.007. Even though FA/B was not significant for compressive strength, it is possible that because it was only at 28 days of curing and not longer. Lack of fit was chosen at a significance level of 0.05. Both responses showed p-values greater than 0.05, demonstrating that the model fits the data. The R^2 values for both the spread percentage and compressive models were 63.93 and 74.88 respectively, demonstrating even more the fit of the model to the data.

Figure 3.8 and Figure 3.9 illustrate the residual plot for Spread Percentage and Compressive Strength (MPa), respectively. The normal probability plot in the residuals approximately follows a straight line indicating the residuals were normally distributed. The residual versus fits plot showed no apparent pattern, having a good distribution between the positive and negative area, which indicates that a linear model provides a useful fit to the data and nearly constant variance. The residual versus order plot also showed no trend at the when displayed in time order, which means that the residuals are independent from one another.

Table 3.6: ANOVA and full regression model statistics

Term	Spread Percentage		Compressive Strength	
	p-value	Coefficients	p-value	Coefficients
Constant		50.6		17.03
G/B	0.472	NSS[a]	0.007	-0.916
FA/B	0.021	-2.219	0.281	NSS
$(G/B)^2$	0.659	NSS	0.111	NSS
$(FA/B)^2$	0.202	NSS	0.428	NSS
G/B*FA/B	0.801	NSS	0.900	NSS
Lack-of-Fit	0.248		0.212	
R^2 (%)		63.93		74.88

[a] NSS: Not statistically significant

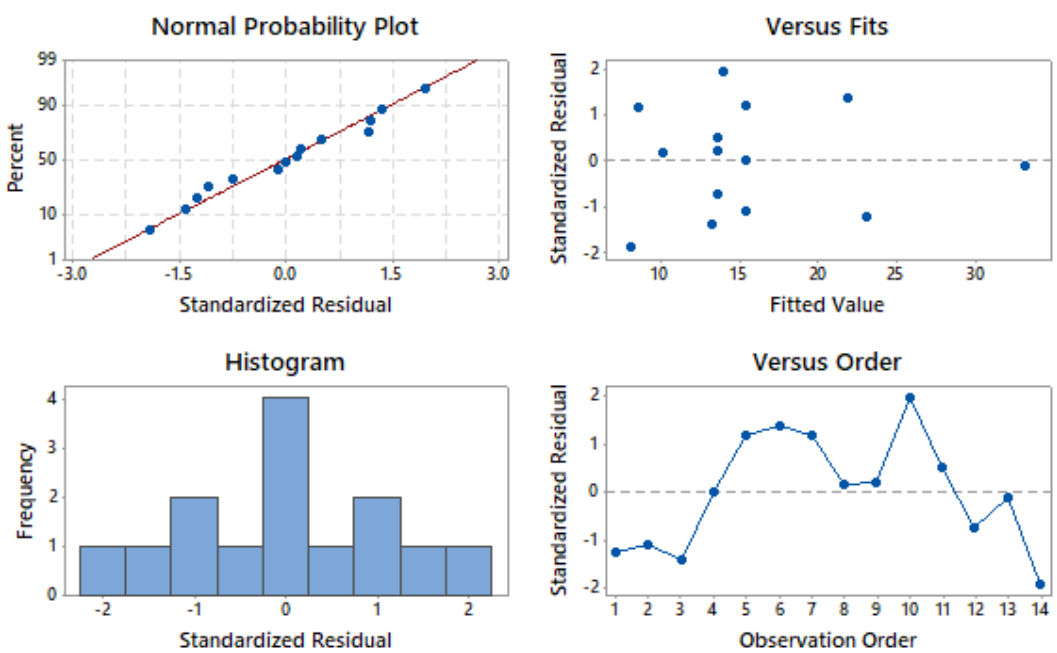

Figure 3.8: Residual plots for Spread Percentage

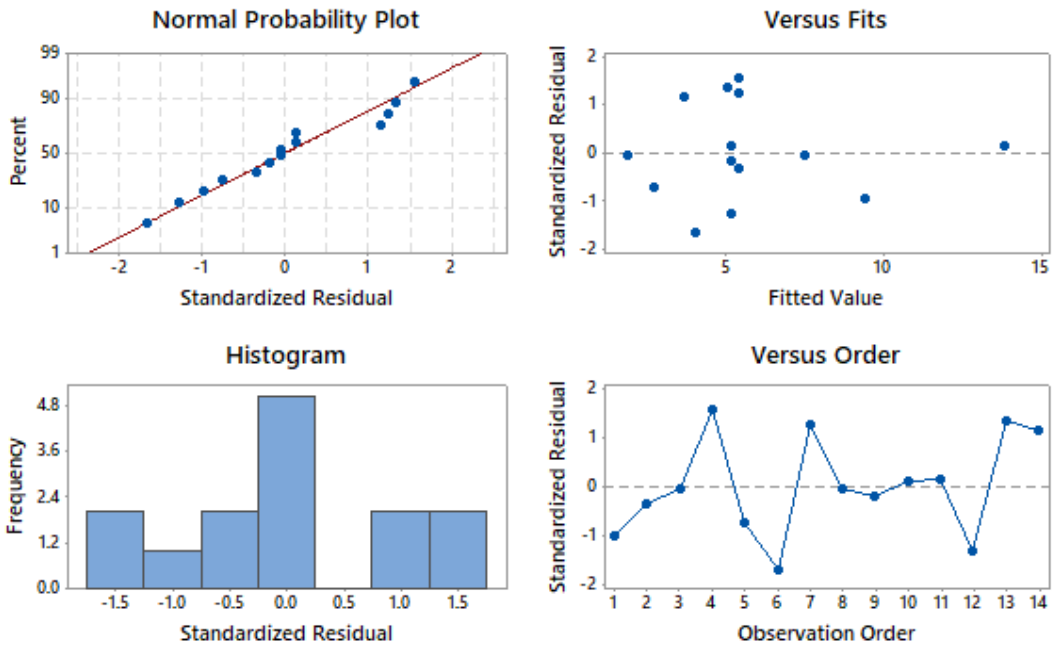

Figure 3.9: Residual Plot for Compressive Strength (MPa)

Given that the main effects and their interaction were analyzed using ANOVA, regression equations on the model for each response can be obtained. Equation 3.1 and Equation 3.2 show the regression equations models for spread percentage and compressive strength as Box-Cox transformations.

$$\frac{SP^{\lambda} - 1}{\lambda g^{\lambda-1}} = 50.6 - 2.219\frac{FA}{B} \tag{3.1}$$

Where λ = 7 and g is the geometric mean = 106.54

$$\frac{{CS_{28}}^{\lambda} - 1}{\lambda g^{\lambda-1}} = 17.03 - 0.916\frac{G}{B} \tag{3.2}$$

Where λ = 11 and g is the geometric mean = 79.30

From both equations 3.1 and 3.2, it can be seen that only the main effects were significantly affecting both responses. For the spread percentage, the linear term of FA/B was the only factor affecting the response significantly. That is, the spread percentage was predicted to decrease with the addition of FA as partial replacement of Portland cement. For compressive strength, on the contrary to spread percentage, only the linear term of G/B was the only factor found to affect the response significantly, although its coefficient was relatively small. In other words, a decrease in glass would have an improvement in the compressive strength.

3.4.3 Response Optimization

The Response Optimizer tool in MiniTab 17 was used to obtain an optimal design that was implemented in the constrained experimental region based on the mixture specifications. Table 3.7 shows the desired goals for each response. A composite desirability of 90% was chosen for both the compressive strength and flow table. Based on that desirability the optimization plot as depicted in Figure 3.10 indicates that maximum compressive strength of 83 MPa and a targeted flow table of 110% can be obtained with a G/B of 7.3% and FA/B of 14.3%.

Table 3.7: Measured and optimization values from the response optimizer tool

Dependent Variable	Measured		Optimization	
	Lower	**Upper**	**Goal**	**Target**
Spread Percentage (%)	86.1	119.3	Target	110
Compressive Strength (MPa)				
28 days	74	84.6	Maximize	83

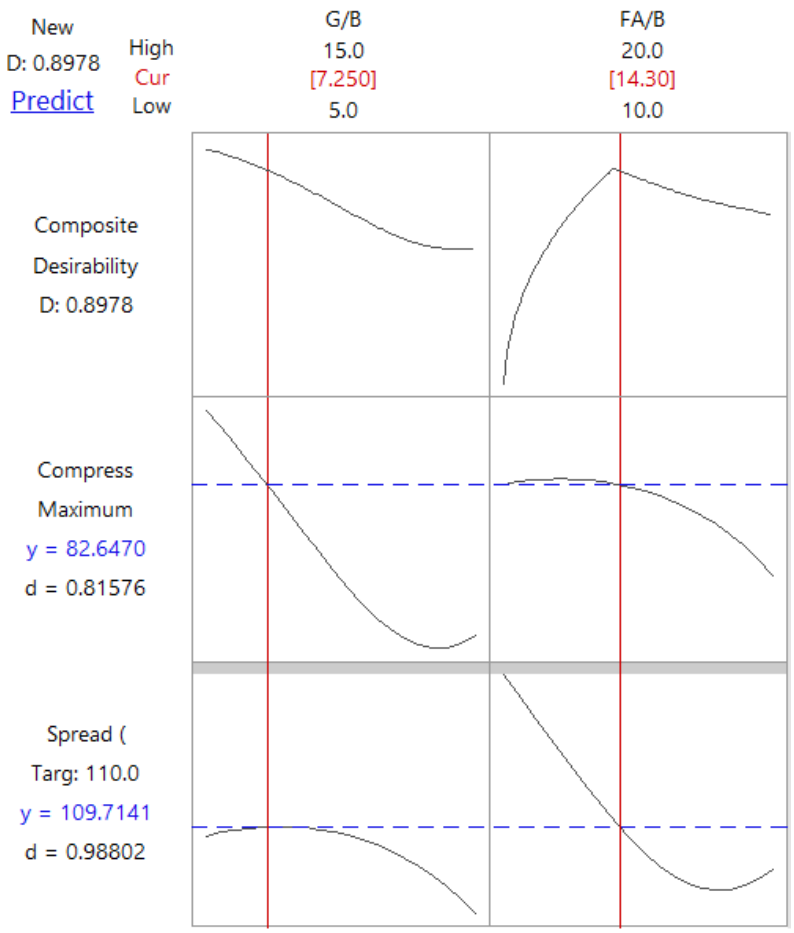

Figure 3.10: Response optimizer plot

3.4.4 Contour Plots

The relationship between the independent and dependent variables (i.e. response) was evaluated with contour plots. Each response was evaluated independently with the predictors plotted in the x- and y-axis. As shown in Figure 3.11, in order to achieve a higher value of the spread percentage response there needs to be a decrease in G/B and FA/B. Thus, the G/B provides a good range in values to obtain a targeted desired spread percentage of 110%. Comparatively, Figure 3.12 shows that in order to increase the compressive strength response, there needs to be a decrease in both G/B and FA/B. Still the FA/B region provides a wide range that can be used to obtain the desired value of 83 MPa. Nevertheless, the decrease values for each independent variable can be attributed to 28 days of curing and not longer.

An overlay plot of spread percentage and compressive strength in function of G/B and FA/B was done to find where the predicted values of the two response variables are within an acceptable range. As a result it allowed the identification of an area of compromise among the responses. For spread percentage the desired range was set between 105 and 115% and for compressive strength the maximum possible range was chosen between 80 and 85 MPa. Figure 3.13 shows the feasible region to obtain the optimum values for the selected ranges in both responses.

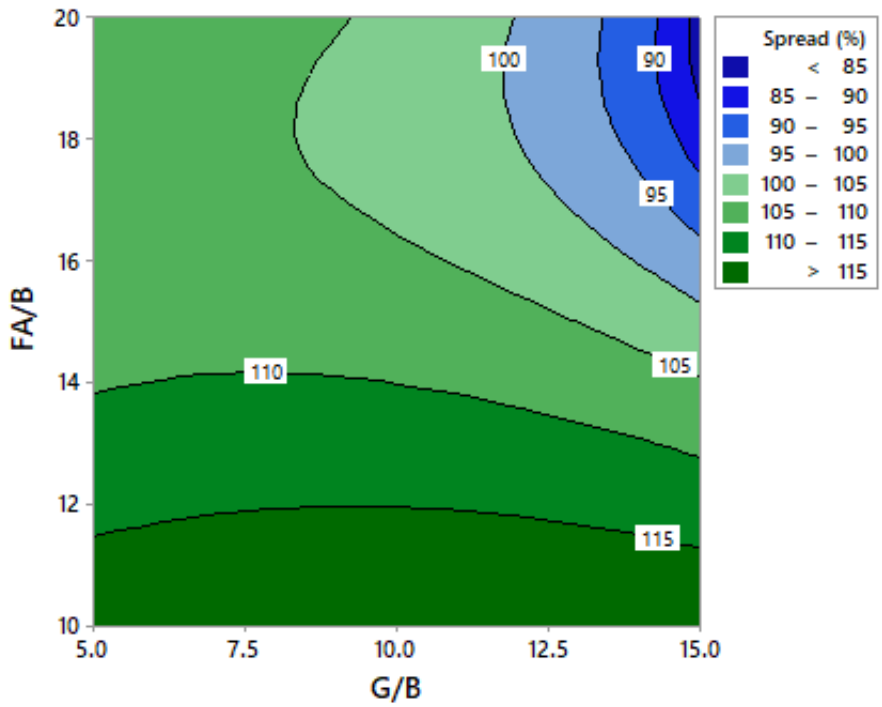

Figure 3.11: Contour Plot of the Spread Percentage in function of FA/B and G/B

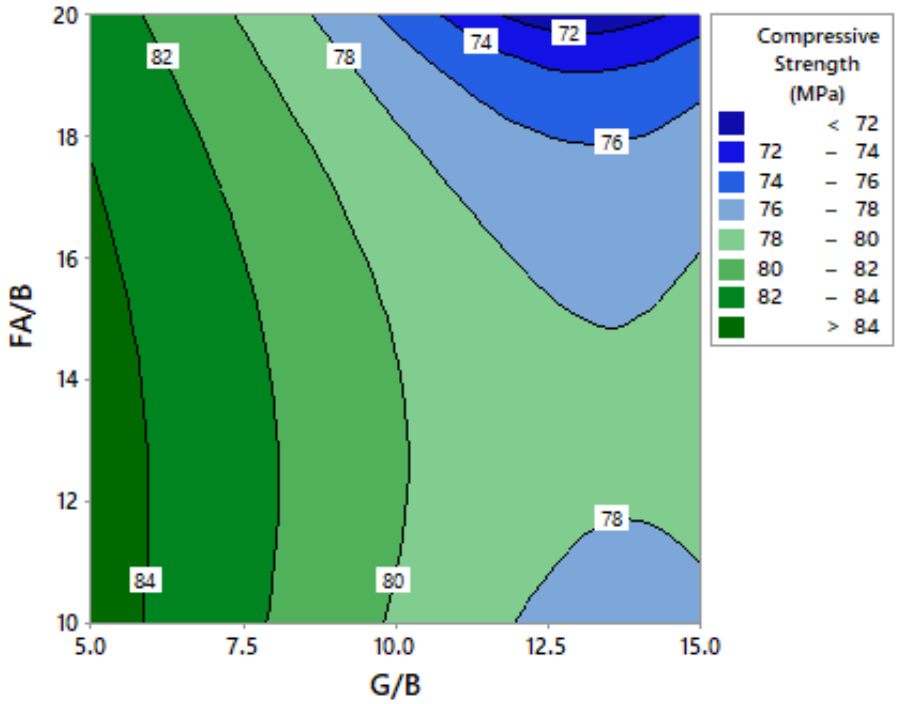

Figure 3.12: Contour Plot for Compressive Strength in function of FA/B and G/B

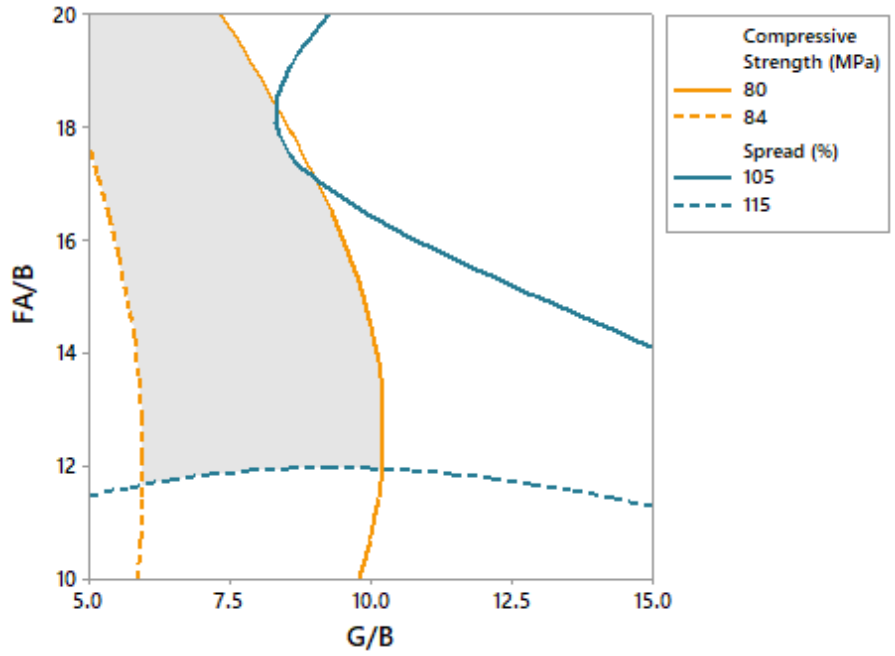

Figure 3.13: Overlaid plot in function of G/B and FA/B

3.4.5 Model Validation

In order to test the accuracy of the model, validation was done by performing a new set of experiments and comparing the results with the predicted values as illustrated in Table 3.8. A spread percentage value of 110% was obtained for the measured response. As predicted by the model, this value fell within the 95% Confidence Interval. Correspondingly, this value was in compliance with ASTM C270, which specifies that the mortar should produce a flow of 110% ± 5. Nevertheless, a measured value of 74 MPa was obtained for the compressive strength response. Even though this result did not fall within the 95% Confidence Interval, the value obtained was 62%, which is higher than the minimum recommended 28 MPa on ASTM C150 for Portland cement.

Table 3.8: Confidence Intervals at 95% predicted by the model

Response	Predicted	Measured	95% CI
Spread (%)	110	110	(101.76, 114.95)
Compressive Strength (MPa)			
28 days	83	74	(81.05, 83.87)

3.4.6 Compressive Strength

Mortar specimens were used to evaluate the compressive strength performance of cement, glass powder and fly ash. The test results of mortar compressive strength for individual samples, mean strengths and standard deviation at 7, 28, 56 and 90 days of curing are tabulated in Table 3.9. Results showed that for 7 days of curing an average compressive strength of 53.8 MPa was achieved. This value is in accordance with ASTM C150, which states that for 7 days and Type 1 Portland cement, a minimum of 19 MPa is required. As previously mentioned in section 3.5.5, for 28 days, the average compressive strength was found to be 74 MPa. This is a 37.5% increase in compressive strength when compared to 7 days result. Kim et al. (2015) investigated the influence of glass powder and fly ash on the compressive strength of mortar. The study reported that at 28 days of curing, the compressive strength of a mortar containing 5% of powder glass was higher than that of a normal Portland cement and 10% FA mortars. The different rate of strength development was associated with finer particle size when compared to

FA. With a larger surface area, the rate of the pozzolanic reaction was improved, leading to higher early strength mortar. Kim et al. (2015) also reported that the combination of 10% glass powder and 10% FA showed the highest compressive strength of all tested mortar mix designs. It was then concluded that the slow strength development of concrete with FA could be enhanced by the incorporation of glass powder as cement replacement in this study. For 56 days of curing, results showed an average compressive strength value of 88.9 MPa. This represents a 20% increment from the value obtained at 28 days. For 90 days of curing, the measured compressive strength was 94.3 MPa.

Table 3.9: Compressive strength test results of mortar

Age (days)	Experimental Test Results (MPa)			Average (MPa)	Standard deviation (MPa)
	Specimen 1	Specimen 2	Specimen 3		
7	53.7	53.4	54.4	53.8	0.5
28	76.3	72.0	73.8	74.0	2.1
56	87.9	87.2	91.9	88.9	2.5
90	95.5	94.1	93.3	94.3	1.1

3.4.7 Splitting Tensile Strength

Splitting Tensile Strength test was done in triplicate at 28 days of curing. An average value of 13.6 MPa was achieved. For normal weight concrete, the average splitting tensile strength is approximately equal to $6.7 * \sqrt{f'_c}$, where f'_C is the compressive strength (ACI, 2011). With a compressive strength value of 74 MPa, the tensile strength value was 64% higher than the recommended value. Even though the result is within typical values, other studies incorporating the use of FA as cement replacement have shown higher values for splitting tensile strength. Soto-Pérez (2015) studied the influence of FA on the mechanical properties of mortar cement pastes. Results from the study showed that with a w/b at 0.30 and a FA replacement at 10 – 20%, the splitting tensile strength ranged from 26 – 32 MPa.

3.5 CHAPTER CONCLUSIONS

The following conclusions can be made based on the results from the optimum PC mix design with glass powder and fly ash as cement replacement by RSM:

- XRD revealed an amorphous pattern on the glass powder
- Hydrometer test results revealed a particle size distribution ranging from 0.07 to 30 µm. The cumulative measure for 50% of the particles size was 8 µm.
- At 28 days of curing, the compressive strength values ranged from 74 to 84.6 MPa and the spread percentage ranged from 86.1 to 119.3%.
- The regression models obtained for both compressive strength and spread percentage response demonstrated to be a linear model. The compressive strength response was found to increase with a decrease in G/B and spread percentage was found to increase with a decrease in FA/B.
- The optimum values for a compressive strength of 83 MPa and 110 spread percentage were 7.25% G/B and 14.30% FA/B.
- Validation demonstrated that spread percentage fell into the 95% Confidence Interval with a measured value of 110%. Even though the compressive strength validation results did not fell into the 95% Confidence Interval, the measured value of 74 MPa was higher than that of normal Portland cement mortar.
- At 28 days of curing, splitting tensile strength was 13.6 MPa.
- At 56 days of curing, compressive strength was 88.9 MPa. That is approximately a 15 MPa increased value when compared to 28 days.
- At 90 days of curing, the measured compressive strength was 94.3 MPa.

4 OPTIMIZED MORTAR APPLICATION TO PERVIOUS CONCRETE

4.1 ABSTRACT

After acquiring an optimized mortar paste with glass powder and FA as cement replacement a study was done to evaluate its performance in pervious concrete. Permeability and Compressive Strength are both important mechanical properties for PC and they are inversely proportional to each other. Achieving a good balance between them is imperative to attain the ideal PC design. At 7 days, the average measured compressive strength for the PC specimen was found to be 11.9 MPa. For 28 days of curing, a permeability of 2.87 mm/s and a compressive strength of 15.2 MPa were measured. Both values fell within the typical ranges specified by the NRMCA. Fine aggregates increased workability while causing a more dense concrete. As the density increases, its compressive strength also increases but simultaneously so does its porosity. The hardened PC specimen showed a measured density of 1,872 kg/m^3 and void content of 25.8%. In the same way it was found that the values for both the density and void content are within the typical values according to ASTM C1754. To measure the PC resistance to degradation, the LA abrasion test as a means of physical durability of PC was performed at 28 days. After 500 revolutions at 30 rpm, results revealed a mass loss percentage of 46%.

4.2 MATERIALS

Portland Cement Type GU conforming to ASTM C150 was used. Fly Ash was obtained from AES Puerto Rico, a local coal-fueled power plant located in the municipality of Guayama (Table 3.1 from Chapter 3). Glass Powder from milled glass bottles was also used as previously mentioned in Chapter 3. Also for admixture as per ASTM C494, MasterMatrix VMA 362 viscosity-modifying admixture (VMA) provided by BASF was used. Limestone gravel in compliance with ASTM D448 and ASTM C33 was used as coarse aggregate and was obtained from a local hardware store. The gravel was sieved to collect a gradation size of 3/8 in. (9.5 mm).

4.3 METHODOLOGY

4.3.1 PC Testing and Validation

A Response Surface Methodology (RSM) was done in Chapter 3 to optimize and validate a 28 days mortar mix design for spread percentage and compressive strength in accordance with ASTM C1437 and ASTM C39, respectively. After testing, the optimal design for a targeted spread percentage of 110% and a compressive strength of 83 MPa were found to be with a G/B of 7.25% and FA/B of 14.3%. With this optimized mortar mix design, a PC mix was tested on compressive strength, permeability and durability at 28 days of curing. The binder-to-aggregate mass ratio was 1:4. Additionally, compressive strength test was also done at 7 days to analyze the strength development over time.

4.3.2 PC Specimen Preparation

The PC specimens were prepared in accordance to ASTM C470. The limestone gravel was not thoroughly cleaned to assimilate field conditions. Following the guidelines on ASTM C192, a mechanical concrete mixing machine was used to prepare the optimized mixture. Tap water available from the laboratory was used for the preparation. Specimens were cast in cylinders with dimensions of 20 cm x 10 cm. Each specimen was compacted following the standard rodding consolidation method. Tools such as sampling and mixing pan, tamping rod, scoops and towels, were also used during the preparation process. Specimens were put in a sealed plastic bag for the first 24 hours to prevent water loss. Subsequently, the specimens were removed from the molds and placed in a tank filled with lime-saturated water at ambient temperature (24 ± 2°C) for the curing process as per ASTM C511.

4.3.3 Permeability Test

For the purpose of measuring the permeability (k), an infiltration test was performed in a constant water head tester. In this approach, the sampled specimen was wrapped with a parafilm membrane to avoid water flowing along the sides of the specimen. Water was added to the column to fill the specimen cell and the draining pipe. The specimen was preconditioned by allowing water to drain out through the pipe until a constant flow was achieved. This ensured

that the specimen was completely saturated with water. After this operation, the volume of water passing through the specimen was measured for approximately 60 sec.

Pervious concrete pavement will typically have an infiltration rate of 340 in/hr. (2.40 mm/s), which is more than 100 times the infiltration rates found in most natural soils (Leming et al., 2007). Table 4.1 shows the typical infiltration rates on based on the general hydrological soil groups.

Table 4.1 Typical infiltration rates for natural soils based on Hydrological Soil Group (NRCS, 1986)

HSG	Soil Texture	Typical Infiltration Rates (in/hr.)
A	sand, loamy sand, sandy loam	< 0.30
B	silt loam, loam	0.15 – 0.30
C	sandy clay loam	0.05 – 0.15
D	clay loam, silty clay loam, sandy clay, silty clay, clay	0 – 0.05

Darcy's Law as shown in Equation 4.1 measured the amount of flow passing through the cylinder at a given time to calculate the permeability.

$$k = \frac{(V_W * L)}{(A * \Delta h * t)} \tag{4.1}$$

Where, k is the permeability (mm/s), V_W is the volume of water collected (mm^3) , L is the length of the specimen (mm), A is the cross sectional area of the specimen (mm^2), Δh is the head difference (mm) and t is the time (sec).

4.3.4 Compressive Strength

PC specimens were tested for compressive strength in accordance to ASTM C39. The samples were cured under limewater for 7, 28 and 56 days and then tested. A 3000 kN Forney universal testing machine was used. To provide a uniform load distribution, capping rubber pads

(Gilson HM-362) were used. Figure 4.1 shows the specimen being tested for compressive strength in the Forney universal testing machine.

Figure 4.1: Forney universal testing machine (left), Compressive strength test on pc specimen (right)

4.3.5 Density and Void Content of Hardened PC

The density and void content of hardened PC were determined according to ASTM C1754. The specimen was dried in an oven at a temperature of 110 ± 5°C for 24 ± 1 h. After allowing the specimen to cool in air at room temperature, the dry mass of the specimen was recorded. Then, the specimen was submerged completely in a water bath for 30 ± 5 min and while keeping the specimen submerged, its mass was determined. To calculate the density of the specimen Equation 4.2 was used.

$$Density = \frac{K * A}{D^2 * L} \tag{4.2}$$

Where K is a conversion factor (1, 273, 240 in SI units), A is the dry mass of the specimen (g), D is the average diameter of the specimen (mm) and L is the average length of the specimen (mm). The void content was determined using Equation 4.3.

$$Void\ Content = \left[1 - \frac{K * (A - B)}{\rho_w * D^2 * L}\right] * 100 \tag{4.3}$$

Where B is the submerged mass of the specimen (g) and ρ_w is the density of water at the temperature of the water bath (kg/m^3).

4.3.6 Los Angeles Abrasion Test

In order to analyze the PC abrasion resistance, the Los Angeles abrasion machine was used to perform the abrasion test in accordance to ASTM C1747. A total of three 10 cm x 10 cm specimens were cured and tested at 28 days. As part of the experimental procedure the initial mass of the specimens was recorded before placing them inside the machine. Commonly, for regular concrete or aggregates the test would require the inclusion of steel spheres during the test. However when testing pervious concrete, these were not included as specified in the aforementioned ASTM. The test was performed for a total of 500 revolutions at a speed of 30 rpm. After 500 revolutions, the final mass of the specimens was recorded. The mass loss percentage was determined with Equation 4.4 where M_i is the initial mass (g), and M_f is the final mass (g).

$$M_{loss}(\%) = \frac{M_i - M_f}{M_i} x\ 100 \tag{4.4}$$

Figure 4.2: LA Abrasion Machine

4.4 RESULTS AND DISCUSSION

4.4.1 Permeability and Compressive Strength

At 28 days of curing, the average permeability of the PC specimen resulted in a value of 2.87 mm/s. Even though this value is within the National Ready Mix Concrete Association (NRMCA) typical permeability ranges (1.4 mm/s – 12.5 mm/s), lower values can be attributed to the casting in cylinders, where the paste can slide to the bottom of the cylinder, which can cause clogging and therefore reduce the infiltration rate of the specimen. Compressive strength of the PC specimen was tested in triplicate for 7 and 28 days and results are shown in Table 4.2. As compressive strength increases, the permeability decreases (ACI, 2010). Although pervious concrete can be designed to attain high compressive strengths, typical values range from 2.8 to 28 MPa (NRMCA, 2004). The average values for compressive strength obtained from both 7 and 28 days, indicates that they are both within compliance. Since higher values for compressive strength were obtained from the optimized mortar mix in Chapter 3, similarly it was expected to achieve higher values for the PC specimen.

Table 4.2: Compressive strength test results of the PC specimens

Age (days)	Experimental Test Results (MPa)			Average (MPa)	Standard deviation (MPa)
	Specimen 1	Specimen 2	Specimen 3		
7	10.7	12.7	12.3	11.9	1.0
28	13.1	18.0	14.6	15.2	2.5

4.4.2 Density and Void Content of Hardened PC

In order to obtain higher values for compressive strength, the PC specimen is expected to be denser. But as density increases, there is a corresponding reduction in porosity and permeability (Kevern et al., 2009). The value for density for the hardened PC was found to be 1,873 kg/m^3. Typical values for PC specimen range from 1650 to 1943 kg/m^3 (ASTM C1754).

The percolation of water is achieved through a series of interconnected voids. As void content increases, the compressive strength decreases (Kevern et al., 2009). The measured void content resulted in a value of 25.8%. As per ASTM C1754, typical values ranged from 22.6 to 37%. Both density and void content results resembled the previous study done by Arocho-Irrizary (2018) who reported density and void content of 1,864 kg/m^3 and 24% respectively.

4.4.3 Los Angeles Abrasion Test

The LA abrasion machine was used to measure the PC's durability. After 500 revolutions the measured mass loss percentage was 45%. PC specimens before and after the test are shown in Figure 4.3. Marines-Muñoz (2012) also studied the abrasion resistance of PC specimens made with slag and three different types of coarse gravels (pea gravel, limestone and recycled concrete aggregate blend). All aggregates had a nominal maximum aggregate size of 9.5 mm and a w/b of 0.3 that remained constant for all mixtures. Results from the study showed different mass loss values for the different types of aggregates and demonstrated that for limestone gravel the average mass loss was 46.1 ± 3.8 % with a porosity of 25.4 ± 2%. Hence, validating that the durability of the PC specimen will depend on its aggregate type and therefore on its porosity.

Figure 4.3: PC specimen before (left) and after (right) the LA abrasion test

4.5 CHAPTER CONCLUSIONS

The following conclusions can be drawn from the optimized mortar mix application to pervious concrete:

- The permeability of the PC specimen at 28 days of curing was 2.87 mm/s.
- Compressive strength of PC specimen at 7 and 28 days of curing was 11.9 and 15.2 MPa respectively.
- The density for hardened PC was found to be 1,873 kg/m^3, which falls into the typical range values as per ASTM C1754.
- The void content value for the hardened PC was 25.8%. Based on ASTM C1754, this value is within the typical range.
- After 500 revolutions at approximately 30 rpm, the measured mass loss percentage for the PC specimen was 45%.

5 PC FIELD IMPLEMENTATION (PRELIMINARY DESIGN)

5.1 ABSTRACT

When implementing PCP systems, several studies need to be conducted in order to obtain an adequate design. Since all the areas to be analyzed have different characteristics, the pervious concrete designs must be adapted for the selected area. Studies that allow knowing and evaluating more in detail what composes the area are of vital importance. Based on this premise, a hydrological study was carried out for the different areas in need of a pervious concrete system. The study was carried out using the NRCS method, which recommends an analysis with a rainfall recurrence of 2 years and duration of 24 hours. Results of the analysis allow knowing the excess of runoff before and after the implementation of a PC system. For the Mangual/Terrace area, with a design of a 10 cm PC layer and a 20 cm base, the final runoff was 1.3 cm which indicates a reduction in excess runoff of 6.1 cm. In addition, a soil study was carried out and revealed that PCA 5 soil has index properties that classify it as silt. Based on both studies, the proposed design for PCA 5 consists of a width of 2.4 meters and a length of 107 meters with two segments in regular concrete. For the thickness of the segments in permeable concrete, the top layer shall have a depth of 10 cm while the base layer will have a depth of 20 cm. As a means for safety between the cyclists and pedestrians that used the current sidewalk between Mangual and Terrace, the design will serve as a bicycle lane for students who commute daily using that route.

5.2 MATERIALS

For the field implementation, materials used are the ones comprising the optimum mix obtained in Chapter 3 and its application to the PC mix design as presented in Chapter 4. A more detailed description on all the materials are discussed in Section 4.2.

5.3 METHODOLOGY

5.3.1 Hydrological Study

When performing a hydrological study, there are two characteristics of a watershed that must be considered. They are: (1) the amount of runoff that can be anticipated from different areas and (2) the amount of infiltration (i.e. the amount of precipitation that will soak into the soil for some given rainfall). Runoff is not only affected by the slope, but also by the type and extent of the vegetation (Leming et al., 2007). In order to analyze the distribution of surface runoff in the different identified sites on Chapter 2, a hydrological study was performed using the Natural Resources Conservation Service (NRCS) method, also referred to as the Curve Number (CN) method. The method estimates total runoff, providing a useful model of overall site behavior that can be used to evaluate the use of pervious concrete pavement systems in a variety of situations. It utilizes a 24-h design storm, rather than the 15- or 30-minute storm used in the Rational method and so it analyzes the behavior of the system and the site under more realistic conditions. By capturing the behavior of the system throughout longer storm duration, explicitly including the significant effects of infiltration and long-term storage capacity of the pervious concrete pavement system, as well as incorporating the effects of both impervious surfaces and other surfaces with a variety of cover, it allows quantifying critical performance characteristics of the entire site (Leming et al., 2007). To estimate the total volume of runoff, Equation 5.1 was applied.

$$Q = \frac{(P - 0.2S)^2}{P + 0.8S} \tag{5.1}$$

Where Q is the total volume of runoff (inches), P is the precipitation (inches) and S is the area (basin) retention (inches). To calculate S, Equation 5.2 is used.

$$S = \frac{1000}{CN} - 10 \tag{5.2}$$

Where CN is the curve number of the site.

As a general guideline, the storage capacity of an active pervious concrete pavement system is designed to accommodate most, if not all, of the site runoff of the 2-year, 24-h rainfall. The NRCS Curve Numbers are used to estimate the runoff of an area or sub-area with a given type of cover, over a given soil, for a given depth of precipitation. A higher CN means more runoff: a CN of 100 means that all rain will result in runoff. CN's are no greater than 98, even for conventional pavements, since some small amount of rainfall will be held by the surface (Leming, et al., 2007). Table 5.1 was used to estimate the CN of various areas with a given type of cover for soils classified, for hydrologic purposes, as Hydrologic Soil Group (HSG) A (sand, loamy sand, or sandy loam), HSG B (silt loam or loam), HSG C (sandy clay loam), or HSG D (clay loam, silty clay loam, sandy clay, silty clay, or clay), as described in Chapter 4. The NRCS web soil survey was used to identify the different types of soil present in the UPRM as shown in Figure 5.1. Table 5.2 illustrates the identified soils and their respective HSG rating classification.

For the watersheds delineation ArcGIS 10.4 was used. The program uses the digital elevation model (DEM) from the area of interest, which creates a 3D representation of the terrain's surface. With the elevation data available, ArcGIS is able to determine the flow direction, flow accumulation and the streams and with that is able to create and delineate the different watersheds present in the area. For the precipitation data for each specific site, NOAA Atlas 14 was used. The precipitation frequency data was chosen for a design storm with a recurrence of 2 years and 24 hours duration.

Table 5.1: Runoff curve number for urban areas (NRCS, 1986)

Cover Description		Curve Number for Hydrologic Soil Group			
Cover Type and Hydrologic Condition	**Average percent impervious area**	**A**	**B**	**C**	**D**
Fully developed urban areas (vegetation established)					
Open space (lawns, parks, golf courses, cemeteries, etc.) [3]:					
Poor Condition (grass cover <50%)		68	79	86	89
Fair Condition (grass cover 50% to 75%)		49	69	79	84
Good Condition (grass cover >75%)		39	61	74	80
Impervious Areas:					
Paved Parking lots, roofs, driveways, etc. (excluding right of way)		98	98	98	98
Streets and roads:					
Paved; curbs and storm sewers (excluding right of way)		98	98	98	98
Paved; open ditches (including right of way)		83	89	92	93
Gravel (including right of way)		76	85	89	91
Dirt (including right of way)		72	82	87	89
Western desert urban areas:					
Natural desert landscaping (pervious area only)		63	77	85	88
Artificial desert landscaping (impervious weed barrier, desert shrub with 1-to-2 inch		96	96	96	96
Urban districts:					
Commercial and business	85	89	92	94	95
Industrial	72	81	88	91	93
Residential districts by average lot size:					
1/8 acre or less (town houses)	65	77	85	90	92
1/4 acre	38	61	75	83	87
1/3 acre	30	57	72	81	86
1/2 acre	25	54	70	80	85
1 acre	20	51	68	79	84
2 acres	12	46	65	77	82
Developing urban areas					
Newly graded areas (pervious area only, no vegetation)		77	86	91	94

Figure 5.1: UPRM soil rating (Source: NRSC web soil survey, 2018)

Table 5.2: UPRM soil symbols and HSG ratings

Unit symbol	Unit name	HSG rating
Ba	Bajura clay	C/D
CoE	Consumo clay, 20 to 40 percent slopes	B
CoF2	Consumo clay, 40 to 60 percent slopes	B
DaD2	Daguey clay, 12 to 20 percent slopes, eroded	B
GPQ	Gravel, pits and quarries	-
MxE	Mucara clay, 20 to 40 percent slopes	D
Lc	Leveled clayey land	-
Lf	Leveled land, frequently flooded	-

5.3.2 Mangual/Terrace Soil Study

As previously discussed and given that Mangual/Terrace was the location with the greatest need for the implementation of a pervious concrete system, it was decided to carry out a study on the type of soil found in the area. The proper functioning of the pervious concrete system depends not only on its capacity of water absorption, but also on the infiltration rate of the soil that supports it. Additionally, as showed in both Figure 5.1 and Table 5.2, the NRCS web soil survey did not assigned a HSG classification for Mangual/Terrace location, hence, supporting the need for a more thorough study on the soil characteristics.

Field and laboratory test were conducted for the identification and characterization of the soil. Field-testing consisted in performing 4 borings with a manual earth auger drill (Figure 5.2) and sampling extraction using a Shelby tube. Laboratory testing consisted in the classification of the soil in accordance with the unified classification system (ASTM C2487).

Figure 5.2: Manual earth auger drill

5.3.3 PCA 5 Design

According to a recent survey, 17% of the UPRM students commute on bicycles, reflecting a 17% increase in bicycle use from 2009. Some areas with the most bicycle use were analyzed and found that the sidewalk between Terrace and Mangual Coliseum was critical. Additionally, the crash history for UPRM between 2013 and 2014 revealed that there were 15 total accidents involving pedestrians and cyclists, 12 of them being cyclists. The number one cause for the accidents was the inadequate facility. Even more, 17% of those accidents were in Mangual/Terrace Area (Soto, 2014). The area currently has a shared-mode with a 7-ft-wide sidewalk that is frequently crowded by pedestrians and cyclists. As a matter of fact, the existing sidewalk is the main route for many UPRM students living in the Terrace residences to access to the main campus on foot or bicycle. The area needs separate pedestrian and bicycle paths in order to accommodate such an increase in bicycle use to ensure safety of the students.

In order to validate and obtain more information about pedestrians and cyclists who use the route daily, a questionnaire was developed as shown in Figure 5.3. Results showed that 100% of the students felt uncomfortable using the sidewalk, whether it was a cyclist or a pedestrian. In addition, the questionnaire also revealed that 100% of the students had witnessed the area and its surroundings being flooded at some point. For this reason, it was decided to create a pervious concrete design for Mangual/Terrace area (namely, PCA 5) that would provide an exclusive route for cyclists, which helps reduce or even prevent possible collisions between pedestrians and cyclists, providing the students with a safer pedestrian sidewalk for daily commute on campus. Pervious concrete will not only play a role in capturing stormwater runoff but also reduce hydroplaning.

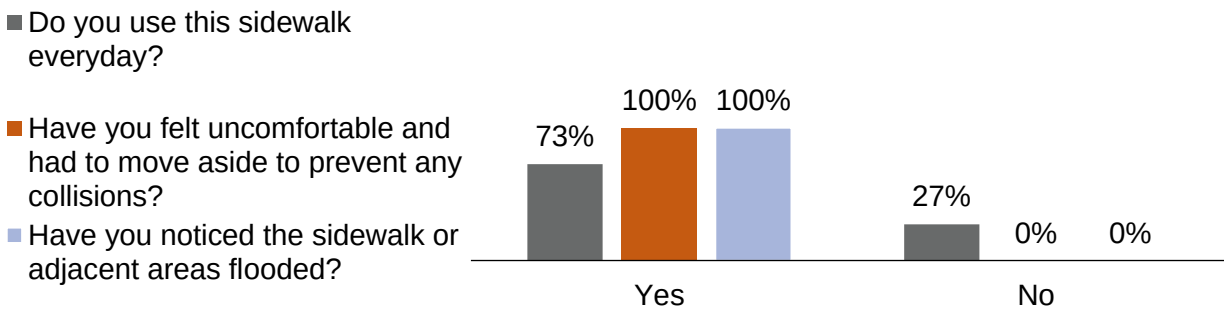

Figure 5.3: Questionnaire results from pedestrians and cyclists

5.4 RESULTS AND DISCUSSION

5.4.1 Hydrological Study

5.4.1.1 Las Palmas Ave.

From ArcGIS it was determined that for Las Palmas Ave. only one watershed forms part of the area as seen in Figure 5.4. The approximate area of the watershed was about 10,682 m^2. The area comprising the watershed was analyzed and it was determined that it consisted of 82% of green areas in good condition, 7% of roofs and 11% of roads, both of which fall under the category of impervious areas. With a D-type soil rating, the curves numbers for green areas, roof and roads were 80, 98 and 98, respectively. Since the watershed has different types of terrain, a weighted average of the curve numbers was used to perform the runoff volume calculation as presented in Table 5.3. Results indicated that for a curve number of 83 and a precipitation of 11.6 cm, the runoff volume was 7.1 cm.

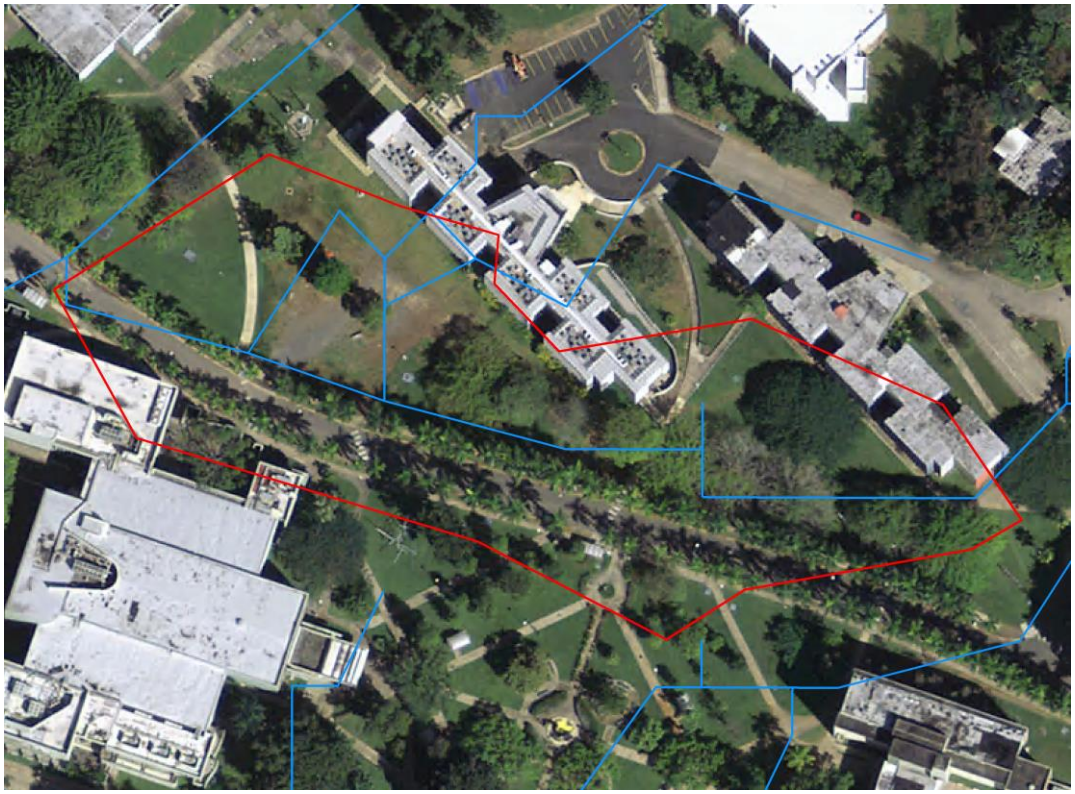

Figure 5.4: Las Palmas Avenue watershed delineation

Table 5.3: Pre-PC implementation CN and runoff for Las Palmas Ave.

Total Watershed Area	HSG	CN (weighted)	Runoff at 2-yr storm (11.6 cm or 4.58 in)
10,682 m^2 (114,980 ft^2)	D	83	7.1 cm (2.80 in)

5.4.1.2 Physics Building

For the Physics building ArcGIS identified three watersheds as part of the area as shown in Figure 5.5. The calculated area for all three watersheds was 10,238 m^2. Additionally, all the area containing the watersheds were analyzed and it was determined that their cover type primarily consisted of green open space areas and impervious areas with roofs and roads. The total area has 24% of green areas in good condition, 70% of roofs and 6% of roads. Since it has a D-type soil rating, the curves numbers for green areas, roof and roads were 80, 98 and 98, respectively. But because the watershed has different types of terrain, a weighted average of the curve numbers was used to perform the runoff volume calculation as presented in Table 5.4. Results showed that for a curve number of 94 and a precipitation of 11.7 cm, the runoff volume was 9.9 cm.

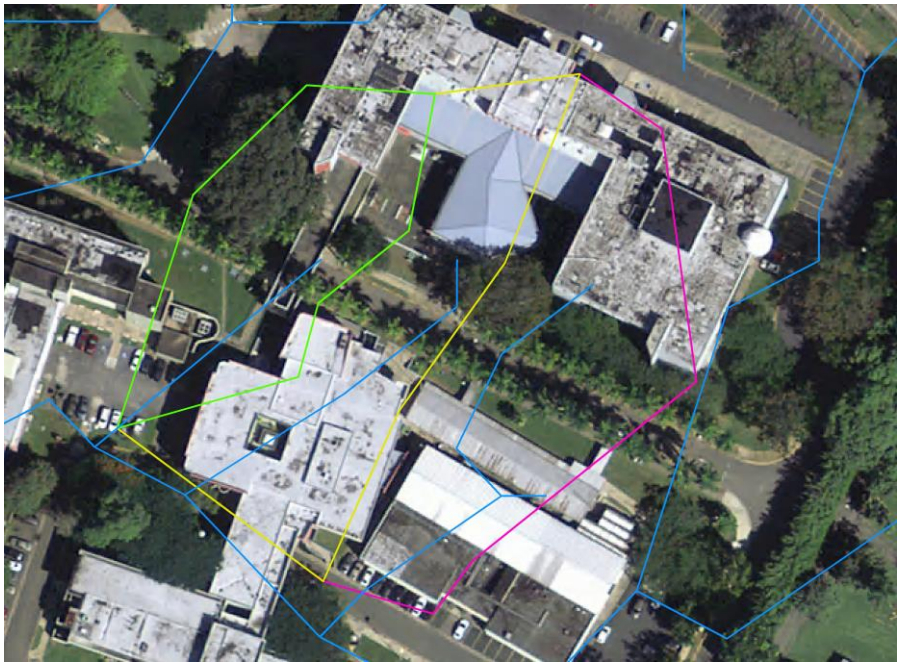

Figure 5.5: Physics building watershed delineation

Table 5.4: Pre-PC implementation CN and runoff for Physics building

Total Watershed Area	HSG	CN (weighted)	Runoff at 2-yr storm (11.7 cm or 4.59 in)
10,238 m^2 (110,201 ft^2)	D	94	9.9 cm (3.90 in)

5.4.1.3 Faculty Building

For the Faculty building, two watersheds were identified part of the area as seen in Figure 5.6. The total measured area for both watersheds was 15,828 m^2. Further analysis on the area, determined that the watershed consisted of 50% of green areas in good condition, 18% of roofs and 32% of roads. The soil rating was found to be D-type giving curves numbers for green areas, roof and roads of 80, 98 and 98 respectively. Nevertheless, because the watershed has different types of terrain, a weighted average of the curve numbers was used to calculate the runoff volume as depicted in Table 5.5. Results showed that for a curve number of 89 and a precipitation of 11.6 cm, the runoff volume was 8.5 cm.

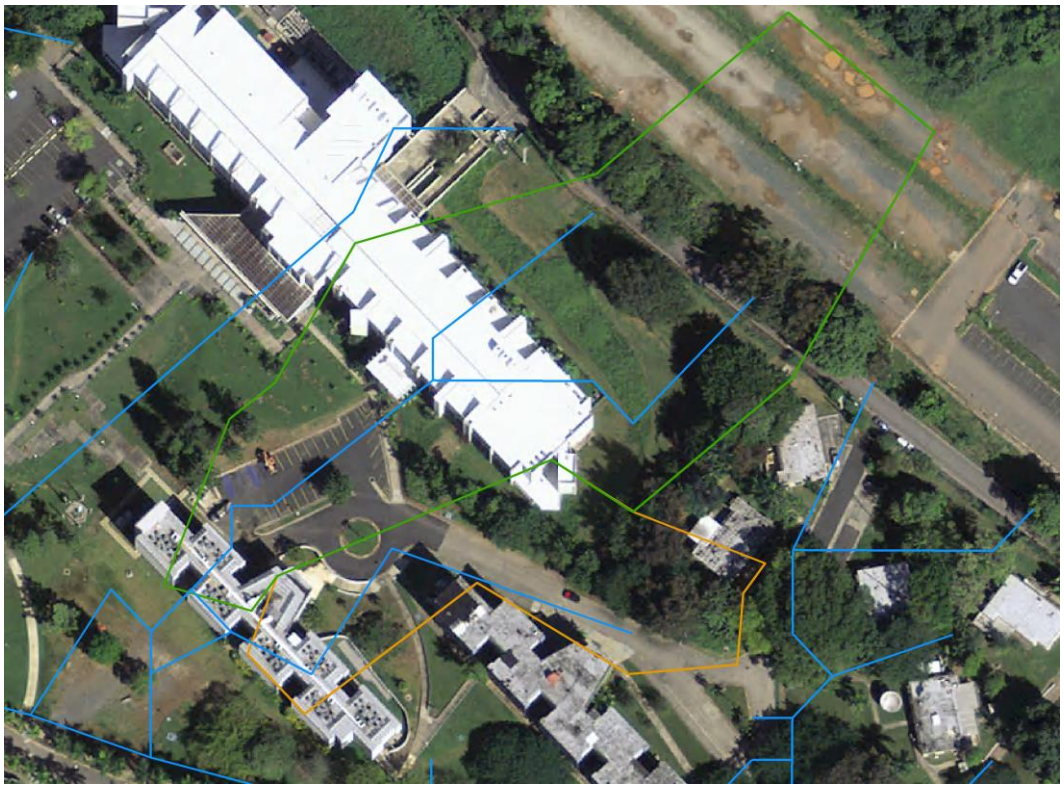

Figure 5.6: Faculty building watershed delineation

Table 5.5: Pre-PC implementation CN and runoff for the Faculty building

Total Watershed Area	HSG	CN (weighted)	Runoff at 2 yr. storm (11.6 cm or 4.56 in)
15,828 m^2 (170,371 ft^2)	D	89	8.5 cm (3.35 in)

5.4.1.4 Nursing Building

The Nursing building had three watersheds as seen in Figure 5.7. The total measured area for all three watersheds was 25,857 m^2. After an analysis of the watersheds, it was determined that the area consisted mostly of 52% of green areas in good condition, 18% of roofs and 30% of roads. Having a D-type soil rating the correspondent curve numbers for green areas, roof and roads were 80, 98 and 98, respectively. However, the watersheds had different types of terrain so in order to calculate the volume runoff, a weighted average of the curve numbers was used as illustrated in Table 5.6. Results indicated that for a curve number of 89 and a precipitation of 11.5 cm, the runoff volume was 8.5 cm.

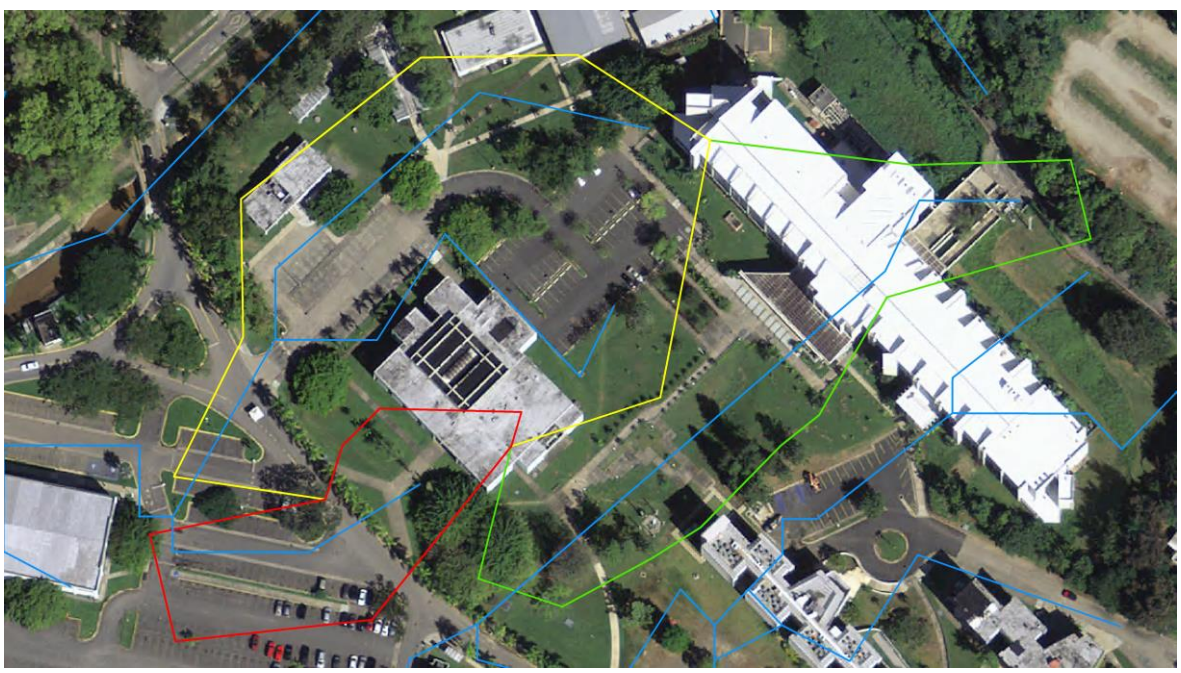

Figure 5.7: Nursing building watershed delineation

Table 5.6: Pre-PC implementation CN and runoff for the Nursing building

Total Watershed Area	HSG	CN (weighted)	Runoff, at 2 yr. storm (11.5 cm or 4.54 in)
25,857 m^2 (278,322 ft^2)	D	89	8.5 cm (3.33 in)

5.4.1.5 Day Care Center

By using ArcGIS, it was determined that the Day care center comprises two watersheds as shown in Figure 5.8. The approximate area for both watersheds was approximately 10,890 m^2. The total area with the two watersheds was analyzed and it was determined that it consisted of 55% green areas in good condition, 10% roofs and 35% of roads. Comparatively, unlike the other identified sites, the Day Care Center had a B-type soil rating. Correspondingly, for this type of rating the curve numbers for green areas, roof and roads were 61, 98 and 98, respectively. The total watershed had different types of terrain. Hence, a weighted average of the curve numbers was used to calculate the runoff volume as presented in Table 5.7. Results showed that for a curve number of 78 and a precipitation of 11.0 cm, the runoff volume was 5.8 cm.

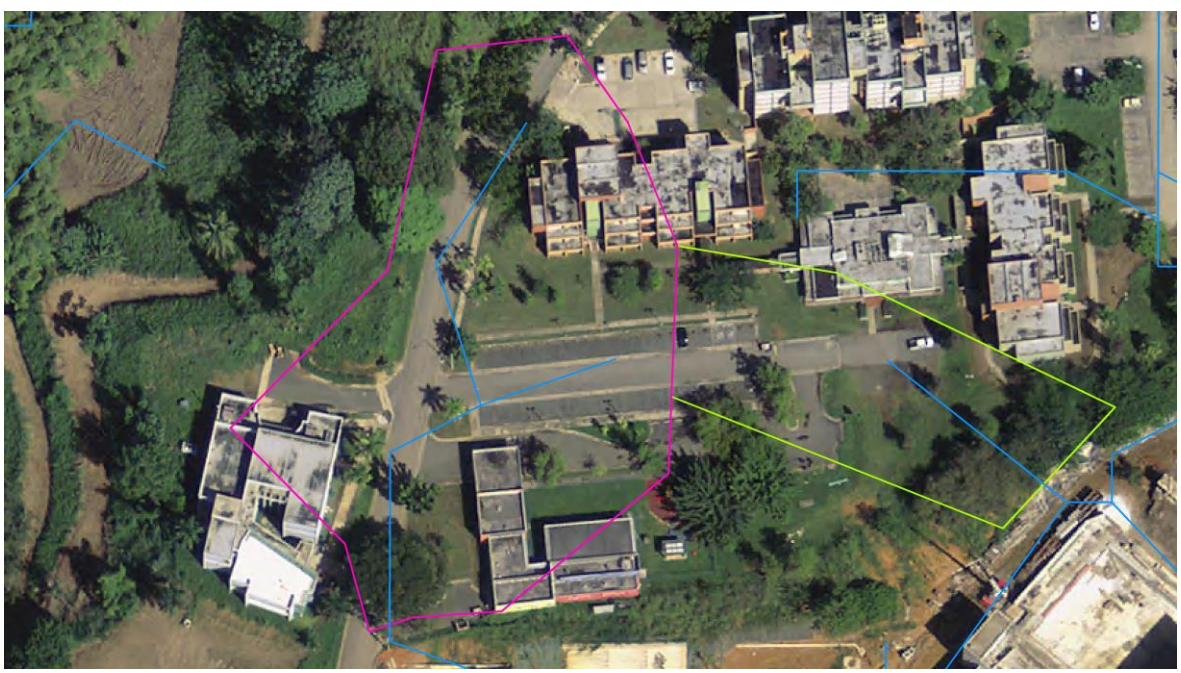

Figure 5.8: Day care center watershed delineation

Table 5.7: Pre-PC implementation CN and runoff for Day care center

Total Watershed Area	HSG	CN (weighted)	Runoff at 2 yr. storm (11.0 cm or 4.34 in)
10,890 m^2 (117,219 ft^2)	B	78	5.8 cm (2.30 in)

5.4.1.6 Mangual/Terrace

For Mangual and Terrace site, three watersheds were identified as depicted in Figure 5.9. The whole area for all three watersheds was approximately 17,581 m^2. The total area consisted of 73% green areas in good condition, 12% roofs and 15% of roads. The soil rating was found to be type D. For this type of rating the curve numbers for green areas, roof and roads were 80, 98 and 98, respectively. With different types of terrains, a weighted average value of the curve numbers was used to calculate the runoff volume as illustrated in Table 5.8. Results showed that for a curve number of 85 and a precipitation of 11.4 cm, the runoff volume was 7.4 cm.

Figure 5.9: Mangual/Terrace watershed delineation

Table 5.8: Pre-PC implementation CN and runoff for Mangual/Terrace

Total Watershed Area	HSG	CN (weighted)	Runoff at 2 yr. storm (11.4 cm or 4.49 in)
17,581 m^2 (189,240 ft^2)	D	85	7.4 cm (2.90 in)

Given that Mangual/Terrace was the identified area in most need for the implementation of PC, a design for it was made. In addition to carrying out a hydrological study of the current state of an area of interest, the NRCS method allows analyzing that study to compare the results of runoff volume once a PC system is implemented. To analyze the study, the rate of infiltration of the soil type present was taken into consideration. In addition, the new analysis involved measuring the depth of the layers of the PC system, as well as the porosity of the gravel used. To carry out the analysis, different base layers with depths of 10 cm, 15 cm and 20 cm and gravel with a porosity of 38% was chosen. For the PC layer, the depth was 10 cm and gravel with a porosity of 25.8% (data obtained in Chapter 4). For soil type D, the infiltration rate chosen within its applicable range was 0.03 cm/hr. It is important to clarify that the post-implementation analysis was carried out for a passive mitigation with 7 days. That is, the analysis measured the amount of runoff excess after 7 days of drawdown. A more detailed description on the design will be further discussed in Section 5.4.3. Table 5.9 shows the results after the implementation of PC, which denoted a final runoff volume of 5.1 cm with a 10 cm base, 3.2 cm with a 15 cm base and 1.3 cm with a 20 cm base.

Table 5.9: Post-PC implementation runoff for Mangual/Terrace

HSG	Infiltration rate	CN	Runoff at 2 yr. storm (11.4 cm or 4.49 in)			
			No base	10 cm (4 in) base	15 cm (6 in) base	20 cm (8 in) base
D	0.03 cm/hr. (0.01 in/hr.)	85	7.4 cm (2.90 in)	5.1 cm (2.00 in)	3.2 cm (1.27 in)	1.3 cm (0.50 in)

5.4.1.7 José de Diego Building

José de Diego building has two watersheds as seen in Figure 5.10. The total measured area for the two watersheds was 7,957 m^2. After an analysis of the watersheds, it was determined that the area consisted mostly of 82% of green areas in good condition, 5% roofs and 13% of roads. Having a D-type soil rating the curve numbers for the green areas, roof and roads were 80, 98 and 98, respectively. Also, because the watersheds had different types of terrain, in order to calculate the volume runoff, a weighted average of the curve numbers was used as showed in Table 5.10. Results indicated that for a curve number of 83 and a precipitation of 11.7 cm, the runoff volume was 7.1 cm.

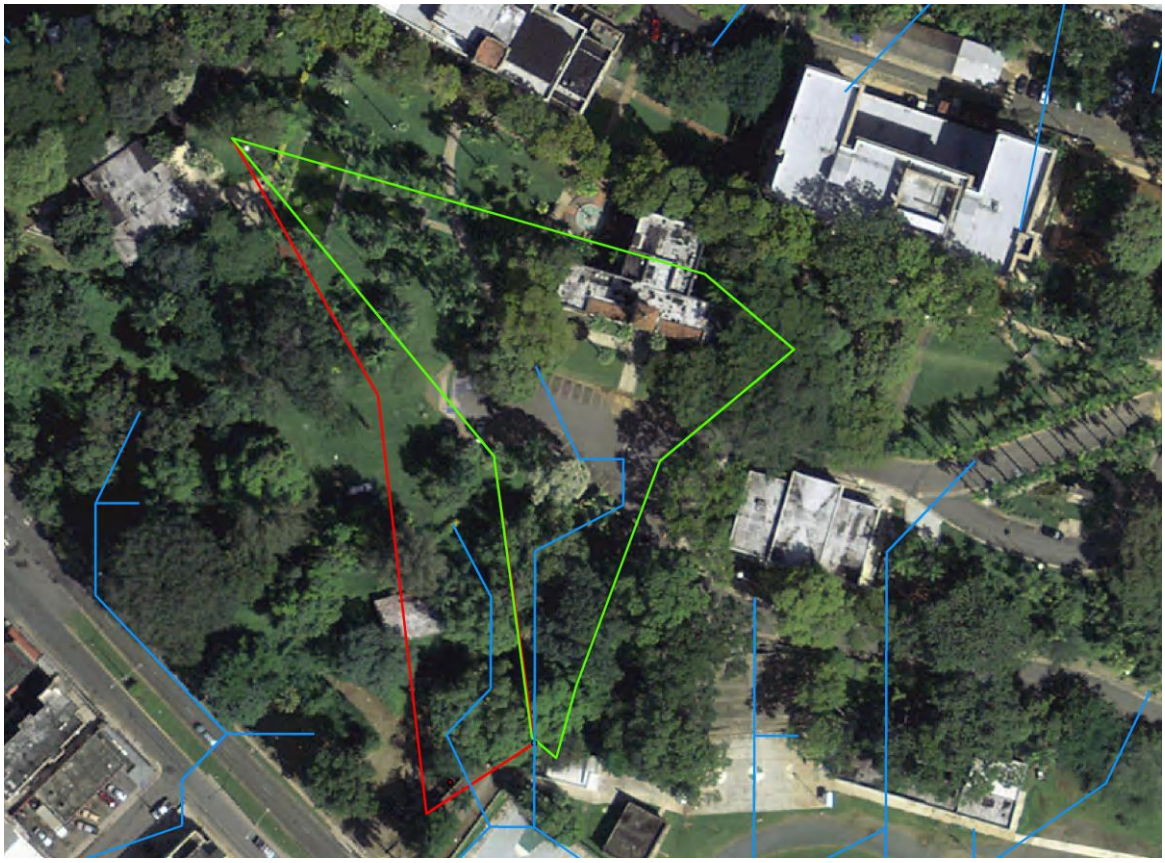

Figure 5.10: José de Diego building watershed delineation

Table 5.10: Pre-PC implementation CN and runoff for José de Diego building

Total Watershed Area	HSG	CN (weighted)	Runoff at 2 yr. storm (11.7 cm or 4.60 in)
7,957 m^2 (85,648 ft^2)	D	83	7.1 cm (2.81 in)

5.4.2 PCA 5 Soil Study

This section is to show the results of the index properties and the classification of the soil found in Mangual/Terrace site. Field test consisted in the drilling of four borings with an average depth of 2.1 m (Figure 5.11). During the drilling operations using the manual auger, the water table was found at 0.9 m from the ground surface. Also, from visual inspection the soil indicated to have a plastic behavior. Figure 5.12 shows the conditions of the soil found at the study site.

Boring	North Coordinates	East Coordinates
1	242,282.37	124,744.44
2	242,282.33	124,743.62
3	242,243.98	124,765.99
4	242,203.81	124,785.93

Figure 5.11: Boring locations and coordinates in NAD 83

Sieve analysis indicated that more than 35% of the material passed the #200 sieve. To be able to classify the soil, the Atterberg limits were measured following the ASTM D4318. The obtained values of Liquid Limit (LL), Plastic Limit (PL) and Plasticity Index (PI) were 71, 44 and 27 respectively. These index properties classified the soil as MH (Elastic Silt) based on the ASTM D2487. As shown on Table 4.1, the NRCS classifies the silt as HSG D, with typical infiltration range values from 0 to 0.17 cm/hr. ACI, 2010 states that where the subgrade infiltration rate is much less than 1.27 cm/hr., the PCP facilitates infiltration and filtering of runoff and recharging of groundwater.

Figure 5.12: Water table (left) and soil extraction (right)

5.4.3 PCA 5 Design

PCA5 estimated dimensions consisted of a width of 2.4 m (8 ft.) and a length of 107 m (350 ft.) with a total area of 260 m^2 (312 yd^2). As it is mainly a bicycle path (i.e., light-weight traffic), the path will be constructed with the optimized pervious concrete mix design obtained from Chapters 3 and 4 and it is proposed to have a thickness of 10 cm, resulting in a total volume of the pervious concrete of 26 m^3 (35 yd^3). The path will be equipped with a gravel layer at a depth of 20 cm under the pervious concrete slab. From the hydrological study on PCA 5, the 20 cm base was chosen since it helps reduce the majority of the surface runoff. This was also due to the fact that the soil infiltration rate was very poorly. Additionally, the gravel layer will serve as a structural support for the pervious concrete slab and also as a temporary stormwater subsurface storage structure. Figure 5.13 shows the design from a top view. It should be noted that the design also contemplates some sections with regular concrete. This is due to the fact that the truck that provides maintenance to the electrical system near the area would have to pass over the proposed project. Thus, the pervious concrete would not be designed to withstand the load of the truck. Figure 5.14 and Figure 5.15 show the cross section for the proposed design and rendering respectively.

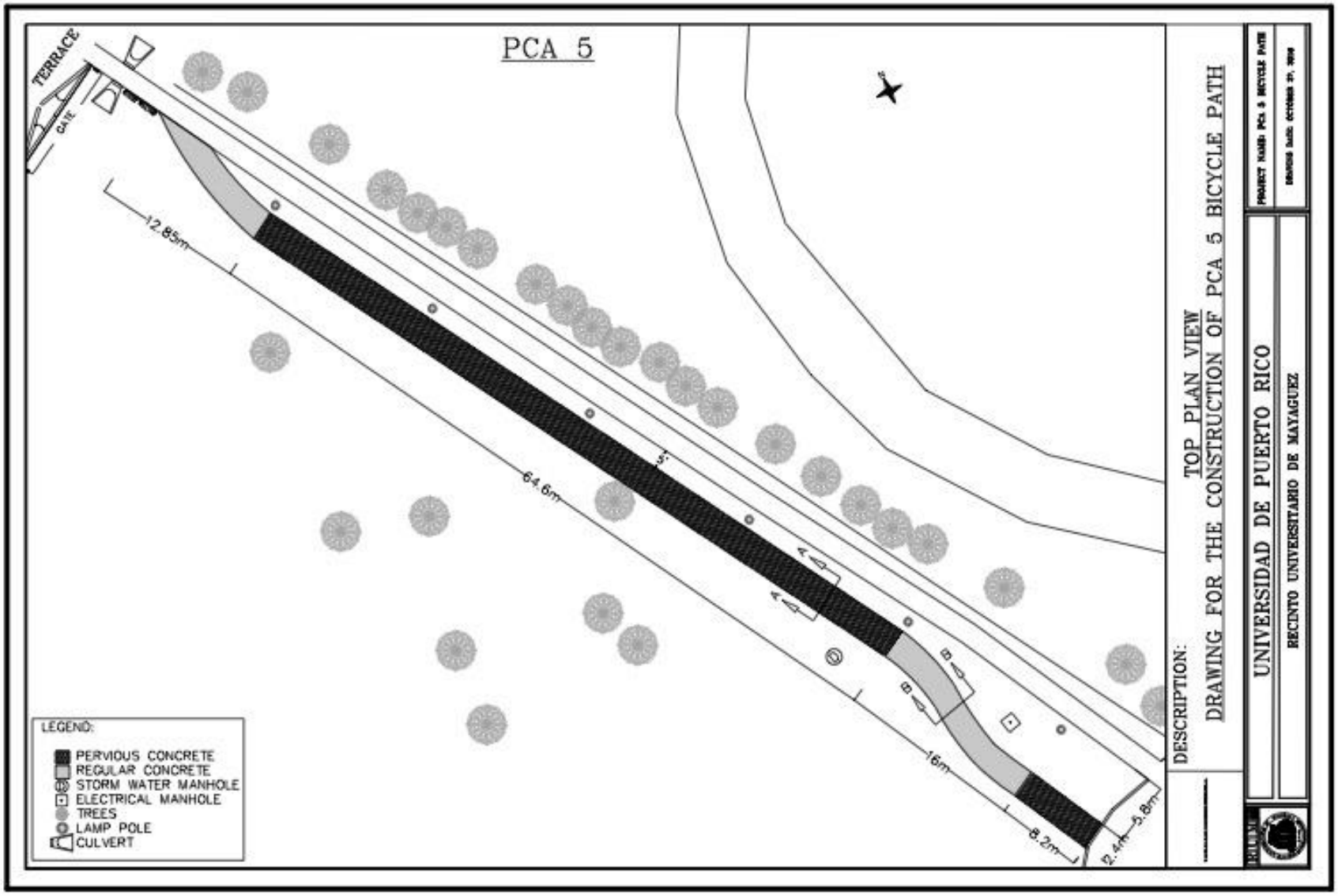

Figure 5.13: PCA 5 top view

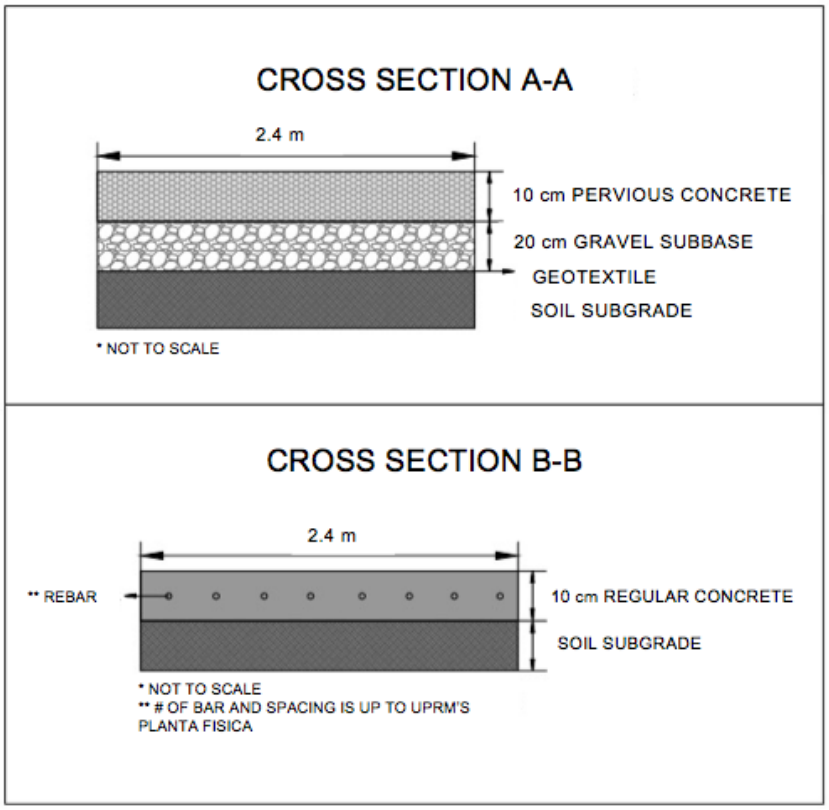

Figure 5.14: PCA cross section

Figure 5.15: Rendering of PCA 5

5.4.4 PCA 5 Construction Cost Estimation

In general, initial costs for pervious concrete pavements are higher than those for conventional concrete or asphalt paving. However, total costs can be substantially lower. Even though the material itself is a little more expensive, pervious concrete is usually thicker than regular concrete. The reason is that the water is going to go through and saturate the subgrade underneath. Therefore, the design needs to address the presence of a weaker subgrade. But when comparing overall installation and life-cycle costs, pervious concrete results in a better option. According to the Center for Watershed Protection, installing traditional curbs, gutters, storm drain inlets, piping, and retention basins can cost two to three times more than low-impact strategies for handling water runoff, such as pervious concrete. Projects that use pervious concrete typically don't need storm sewer ties-ins, which eliminates the cost of installing underground piping and storm drains. Pervious concrete also reduces the need to rebuild storm sewer systems when new developments are built and also increases land utilization, and have a life expectancy equal to the one of regular concrete (Concrete Network, 2018). As previously mentioned pervious concrete initial costs are higher than regular concrete for both material and installation. A comparison in these values was made for typical pervious concrete versus Hwang Eco-friendly Development for Green Environment (HEDGE). HEDGE is a pervious concrete group at UPRM composed of graduate and undergraduate students dedicated to its research and development. Typical cost values for the construction of pervious concrete for material and installation are \$43/m^2 and \$86/m^2 respectively. For HEDGE, the material cost is approximately \$32/m^2 while as for the installation the value is \$65/m^2. Based on the proposed design dimensions, Table 5.11 shows the costs values for both the typical and HEDGE constructions. Even though these values may seem high, since HEDGE works with students and several collaborators, both material and installation costs can be reduced.

Table 5.11: Typical versus HEDGE construction costs for pervious concrete

Item	Averaged Cost for 10 - 20 cm (4 - 8 in) Pervious Concrete	
	Typical	HEDGE
Material	\$11,180	\$8,320
Installation	\$24,682	\$16,900

5.5 Chapter Conclusions

The following conclusions can be made from the PC design phase and its potential implementation as PCA 5:

- Recent surveys revealed the need for the implementation of a bicycle path that separates both cyclists and pedestrian from the current sidewalk between Mangual and Terrace.
- Results from the hydrological study showed that for Mangual/Terrace area, and a design storm with a recurrence of 2 years 24 hours, a PC layer of 10 cm and a base layer of 20 cm produce an excess runoff of 1.3 cm. Hence, producing a reduction of 6.1 cm in the surface excess runoff.
- The soil study revealed that from evaluating the index properties (i.e., Atterberg limits), PCA 5 is classified as MH (Elastic Silt).
- PCA 5 dimensions consisted of a 2.4 m width and 107 m in length. For its thickness, the proposed pervious concrete layer and base will have 10 cm and 20 cm respectively.
- PCA 5 construction costs are lower when compared with HEDGE versus typical values. Even though the initial cost of construction with pervious concrete is higher when compared to regular concrete, when evaluating in a long-term timeframe, pervious concrete results in more benefits than regular concrete.

6 CONCLUSIONS

For the sustainability assessment, the MCDA and the AHP were applied. According to experts surveyed on the seven criteria, the criterion with the highest value turned out to be the impact on daily activities. On the contrary, the criterion with the lowest value was the presence of a nearby stormwater drainage system. After analyzing the three sustainability categories based on the results obtained for the criteria, it was found that the one with the utmost weight was the social sustainability. Results from the criteria analysis also allowed the evaluation of the different areas within the UPRM campus that have the greatest need for a pervious concrete implementation. Mangual/Terrace and the Faculty Building were the most in need. Additionally, results provided support and demonstrated the utility of the AHP when used in combination with the MCDA to obtain an objective approach.

In continuing with the approach of the incorporation of sustainability in the UPRM, it was possible to include solid waste management strategies in the preparation of the optimum mixture of pervious concrete. The inclusion of glass powder and fly ash as a partial replacement of cement helps to reduce and alleviate the costs of disposing them in landfills. Moreover, by including the glass powder and fly ash as part of the mortar mix, tests results for the mechanical characteristics (i.e. compressive strength and tensile strength) were higher than those obtained with a regular mortar of Portland cement. This demonstrates the possible reutilization of both materials in the construction industry. In the same way, the results for compression and permeability of permeable concrete specimens fell within the typical ranges established by the NRMCA and the ACI. Hydrological and soil studies were conducted for Mangual/Terrace area. Results from the hydrological study revealed that the implementation of pervious concrete in the area has the capacity to significantly reduce surface runoff. Similarly, results from the soil study demonstrated that implementing a pervious concrete system would increase the infiltration of runoff water, since the type of soil found in the area has a poor infiltration rate. The proposed design for the Mangual/Terrace area contemplates the construction of a bicycle lane in combination with pervious concrete and regular concrete. This arrangement is expected to reduce collisions between pedestrians and cyclists who currently use the sidewalk for their daily commute, and therefore improving the student's life.

7 RECOMMENDATIONS AND LIMITATIONS

To further expand the investigation, it is recommended to carry out a field demonstration in such a way to measure the rate of in-place infiltration. Also, the ability of the pervious concrete system to remove pollutants from water could be researched. For better characterization of milled glass powder and its influence on concrete chemistry, X-ray fluorescence and an alkali-silica reaction tests are recommended, respectively.

Due mainly to sophisticated installation technique and intensive maintenance, pervious concrete pavement may be more costly than an ordinary concrete pavement. However, social, economic and environmental benefits of the reduction in frequent flash flooding that pervious concrete system will bring in the long run would offset the initial construction cost and operating & maintenance costs.

8 REFERENCES

ACI Committee 522. (2010). Report on Pervious Concrete: (ACI 522R-10). Farmington Hills: MI. American Concrete Institute.

ACI Committee 318. (2011). Building Code Requirements for Structural Concrete: (ACI 318-11) and commentary. Farmington Hills: MI. American Concrete Institute.

AES Puerto Rico (2016). Quienes Somos. *AES*. Retrieved from http://aespuertorico.com/quienes-somos

Almusallam, T.H. (1995). Effect of fly ash on the mechanical properties of concrete. *Proceedings of the 4th Saudi Engineering Conference*. 2, 187–192.

ASTM International. (2016). ASTM C33: Standard Specification for Concrete Aggregates. West Conshohocken, PA: American Society for Testing Materials.

ASTM International. (2016). ASTM C39: Standard Test Method for Compressive Strength of Cylindrical Concrete Specimens. West Conshohocken, PA: American Society for Testing Materials.

ASTM International. (2017). ASTM C150: Standard Specification for Portland cement. West Conshohocken, PA: American Society for Testing Materials.

ASTM International. (2016). ASTM C192: Standard Practice for Making and Curing Concrete Test Specimens in the Laboratory. West Conshohocken, PA: American Society for Testing Materials.

ASTM International. (2014). ASTM C270: Standard Specification for Mortar for Unit Masonry. West Conshohocken, PA: American Society for Testing Materials.

ASTM International. (2017). ASTM C494: Standard Specification for Chemical Admixtures for Concrete. West Conshohocken, PA: American Society for Testing Materials.

ASTM International. (2017). ASTM C496: Standard Test Method for Splitting Tensile Strength of Cylindrical Concrete Specimens. West Conshohocken, PA: American Society for Testing Materials.

ASTM International. (2013). ASTM C511: Standard Specification for Mixing Rooms, Moist Cabinets, Moist Rooms and Water Storage Tanks Used in the testing of Hydraulic Cements and Concretes. West Conshohocken, PA: American Society for Testing Materials.

ASTM International. (2017). ASTM C618: Standard Specification for Coal Fly Ash and Raw or Calcined Natural Pozzolan for Use in Concrete. West Conshohocken, PA: American Society for Testing Materials.

ASTM International. (2013). ASTM C1747: Standard Test Method for Determining Potential Resistance to Degradation of Pervious Concrete by Impact and Abrasion. West Conshohocken, PA: American Society for Testing Materials.

ASTM International. (2012). ASTM C1754: Standard Test Method for Density and Void Content of Hardened Pervious Concrete. West Conshohocken, PA: American Society for Testing Materials.

ASTM International. (2017). ASTM C7928: Standard Test Method for Particle-Size Distribution (Gradation) of Fine Grained Soils Using the Sedimentation (Hydrometer) Analysis. West Conshohocken, PA: American Society for Testing Materials.

ASTM International. (2017). ASTM D448: Standard Classification for Sizes of Aggregate for Road and Bridge Construction. West Conshohocken, PA: American Society for Testing Materials.

ASTM International. (2017). ASTM D2487: Standard Practice for Classification of Soils for Engineering Purposes (Unified Soil Classification System). West Conshohocken, PA: American Society for Testing Materials.

ASTM International. (2017). ASTM D4318: Standard Test Method for Liquid Limit, Plastic Limit and Plasticity Index of Soils. West Conshohocken, PA: American Society for Testing Materials.

Arocho, Irrizary, M. (2018). *Pervious concrete: lab-scale optimization and field application*. Master Thesis, University of Puerto Rico at Mayagüez, PR.

Autoridad de Desperdicios Sólidos (ADS). (2014). Reciclaje en Puerto Rico. *Mapa Interactivo* Retrieved from http://www.ads.pr.gov/ads/mapas/mapa-reciclaje.html

Ayhan, M. B. (2013). A Fuzzy AHP Approach for Supplier Selection Problem: A Case Study in a Gearmotor Company. *International Journal of Managing Value and Supply Chains (IJMVSC)*, *4*(3), 11–23.

Ayub, T., Khan, S. U., & Memon, F. A. (2014). Mechanical characteristics of hardened concrete with different mineral admixtures: A review. *The Scientific World Journal*, *2014*. 1-15.

Basiago, A. D. (1999). Economic, Social, and Environmental Sustainability in Development Theory and Urban Planning Practice. *The Environmentalist*, *19*, 145–161.

Blissett, R. S., & Rowson, N. A. (2012). A review of the multi-component utilisation of coal fly ash. *Fuel*, *97*, 1–23.

Bogena, H. (2015). Water and Sustainable ENERGY. *UN-Water Decade Programme on Advocacy and Communication (UNW-DPAC)*, 1–6.

Cabala, P. (2010). Using The Analytic Hierarchy Process in Evaluating Decision Alternatives. *Operations Research and Decisions*, *1*(1), 6–23.

Castro-Fresno, D., Andrés-Valeri, V. C., Sañudo-Fontaneda, L. A., & Rodriguez-Hernandez, J. (2013). Sustainable drainage practices in Spain, specially focused on pervious pavements. *Water (Switzerland)*, *5*(1), 67–93.

Clean Washington Center. (2016). Chemical Composition of Container Glass. 1-2.

Colantonio, A. (2011). Social sustainability: exploring the linkages between research, policy and practice. *European Research on Sustainable Development*, *1*(1), 35–57.

Concrete Network (2018). Economic Benefits. *Benefits of Pervious Pavements*. Retrieved from https://www.concretenetwork.com/pervious/economic_benefits.html

ECOSOC. (2017). Progress towards the Sustainable Development Goals: Report of the Secretary General, (June), 1–19.

Institutional Office of Research and Planning. (2015). Matrícula General Subgraduada y Graduada 1er semestre 2015 - 2016. Retrieved from http://www.uprm.edu/oiip/estu_a_matricula.html#ano%202015

Islam, G. M. S., Rahman, M. H., & Kazi, N. (2017). Waste glass powder as partial replacement of cement for sustainable concrete practice. *International Journal of Sustainable Built Environment*, *6*(1), 37–44.

Kevern, J.T., Schaefer, V. & Wang, K. (2009). Design of Pervious Concrete Mixture. *National Pervious Concrete Pavement Association*, *3*(1), 13-21.

Khan, M. A. (1995). Sustainable development: The key concepts, issues and implications. Keynote paper given at the international sustainable development research conference, 27–29 march 1995, Manchester, UK. *Sustainable Development*, *3*(2), 63–69.

Kim, J., Yi, C., & Zi, G. (2015). Waste glass sludge as a partial cement replacement in mortar. *Construction and Building Materials*, *75*, 242–246.

Leming, M. L., Malcom, H. R., & Tennis, P. D. (2007). *Hydrologic Design of Pervious Concrete*. Skokie, IL: Portland cement Association.

Lin, Y. H., Tyan, Y. Y., Chang, T. P., & Chang, C. Y. (2004). An assessment of optimal mixture for concrete made with recycled concrete aggregates. *Cement and Concrete Research*, *34*(8), 1373–1380.

Marines, Muñoz, A. (2012). *Evaluation of Sustainability, Durability and the Effect of Specimen Type in Pervious Concrete Mixtures*. Master Thesis, Texas State University at San Marcos, TX.

Montgomery, D. C. (2012). *Design and Analysis of Experiments*. *Design*. Hoboken, NJ: John Wiley & Sons, Inc.

Mtarfi, N. H., Rais, Z., Taleb, M., & Kada, K. M. (2017). Effect of fly ash and grading agent on the properties of mortar using response surface methodology. *Journal of Building Engineering*, *9*(May 2016), 109–116.

Mukharjee, B. B., & Barai, S. V. (2014). Statistical techniques to analyze properties of nano-engineered concrete using Recycled Coarse Aggregates. *Journal of Cleaner Production*, *83*, 273–285.

Nassar, R., & Soroushian, P. (2012). Strength and durability of recycled aggregate concrete containing milled glass as partial replacement for cement. *Construction and Building Materials*, *29*, 368–377.

National Weather Service Forecast Office (NWSF). (2010). Puerto Rico Mean Annual Rainfall. Retrieved from http://www.srh.noaa.gov/sju/?n=climo_annual01

Ng, P. - L., Kwan, A. K. - H., & Li, L. G. (2016). Packing and film thickness theories for the mix design of high-performance concrete. *Journal of Zhejiang University-SCIENCE A*, *17*(10), 759–781.

NOAA. (2014). Point Precipitation Frequency Estimates. Retrieved from https://hdsc.nws.noaa.gov/hdsc/pfds/pfds_map_pr.html

NRCS. (1986). Urban Hydrology for Small Watersheds TR-55. *USDA Natural Resource Conservation Service Conservation Engineering Division Technical Release 55*, 164.

NRMCA. (2004). CIP 38 - Pervious Concrete. *Concrete in Practice. What, why and how?* Silver Springs, MD. National Ready Mix Concrete Association.

Pavlovskaia, E. (2013). Using Sustainability Criteria in Law. *International Journal of Environmental Protection and Policy*, *1*(4), 76-78.

Pratt, C., Wilson, S., & Cooper, P. (2002). Source control using constructed pervious surfaces: Hydraulic, structural and water quality performance issues. *C582*. Construction Industry and Research and Information Association (CIRIA).

Puerto Rico Climate Change Council (PRCCC). (2013). Puerto Rico's State of the Climate 2010-2013: Assessing Puerto Rico's Social- Ecological Vulnerabilities in a Changing Climate. Puerto Rico Coastal Zone Management Program, Department of Natural and Environmental Resources, NOAA Office of Ocean and Coastal Resource Management.

Saaty, T. L. (2008). Decision making with the analytic hierarchy process. *International Journal of Services Sciences*, *1*(1), 83-98.

Saha, A. K. (2017). Effects of class F fly ash on the durability properties of concrete. *Sustainable Environment Research*, *27*, 1–7.

Sahoo, P. K., Kim, K., Powell, M. A., & Equeenuddin, S. M. (2016). Recovery of metals and other beneficial products from coal fly ash: a sustainable approach for fly ash management. *International Journal of Coal Science and Technology*, *3*(3), 267–283.

Sierra, L. A., Pellicer, E., & Yepes, V. (2017). Method for estimating the social sustainability of infrastructure projects. *Environmental Impact Assessment Review*, *65*(February), 41–53.

Soto, D. (2014). *Campus Bicycle Master Plan University of Puerto Rico Mayagüez Campus Bicycle Master Plan*. Mayagüez, PR. University of Puerto Rico at Mayagüez.

Soto, Pérez L. (2015). Optimization of Pervious Concrete incorporating coal fly ash, iron-oxide nanoparticles and water reducing admixtures and its application for the removal of nutrients and fecal coliforms. Master Thesis, University of Puerto Rico at Mayagüez, PR.

US EPA (1993). *Handbook: Urban Runoff Pollution Prevention and Control Planning*. Cincinnati, OH. Office of Research and Development, Center for Environmental Research Information

US EPA (2004). The Use of Best Management Practices (BMPs) in Urban Watersheds. Retrieved from http://purl.access.gpo.gov/GPO/LPS112580

US EPA (2017). Sustainability and the ROE, What is Sustainability? Retrieved from https://cfpub.epa.gov/roe/sustainability.cfm

Wilcox, J., Nasiri, F., Bell, S., & Rahaman, M. S. (2016). Urban water reuse: A triple bottom line assessment framework and review. *Sustainable Cities and Society*, *27*, 448–456.

Zhang, L., Xu, Y., Yeh, C. H., Liu, Y., & Zhou, D. (2016). City sustainability evaluation using multi-criteria decision making with objective weights of interdependent criteria. *Journal of Cleaner Production*, *131*, 491–499.